J. Solid Mech. 2025; 17(04): Article 17

Journal of Solid Mechanics

https://doi.org/10.57647/jsm.2025.1704.17

Research Article

Predicting One-Way slabs' Shear Capacity Subjected to Concentrated Loading Using ANN-Based Formulation

Ali Asghar Akbari Bargoshadi, Ashkan Khodabandehlou*, Fedra Ashrafzadeh, Peyman Hamidi

Department of Civil Engineering, Ur.C., Islamic Azad University, Urmia, Iran

***Corresponding author:** a.khodabandehlou@iau.ac.ir

Article History:

Received:
07 June 2025

Revised:
18 October 2025

Accepted:
28 November 2025

Published in Issue:
31 December 2025

Abstract

The main goal of this study is to present a neural network-based relationship to predict the shear capacity of one-way slabs under concentrated loads. For this purpose, after modeling 5 one-way slabs with different dimension ratios (between 2 and 3.33) by ETABS, the shear capacity of the slab for applying concentrated load along the long span (for eleven different positions) was calculated and the maximum deflection created in the slab was compared and controlled with the allowed value of the codes. After training the optimized neural network, using data obtained from ETABS, the shear capacity of slabs was predicted by MATLAB and the accuracy of this prediction was checked using the regression coefficient. Then, using data fitting and linear regression, the general equation for bearing capacity of the concrete slab in terms of the location of the concentrated load (α) was determined. Finally, in order to determine the accuracy of the presented equation, the real shear capacity of a one-way slab was calculated and compared with the numerical value obtained from the proposed equation. The obtained results indicate the acceptable accuracy of the proposed equation which could predict the shear capacity of the slabs by 96.39%.

Keywords: Concrete slab, One-way, Shear capacity, Neural network, Regression

Cite this article: Akbari Bargoshadi, A.A., Khodabandehlou A., Hamidi, P. & Ashrafzadeh, F., (2026). Predicting One-Way slabs' Shear Capacity Subjected to Concentrated Loading Using ANN-Based Formulation, *Journal of Solid Mechanics,* 17(04): Article 17.
https://doi.org/10.57647/Jsm.2025.1704.17

1. Introduction

Safe structural operation becomes more important as the age of the structure increases. Therefore, the existing structures must be accurately assessed to ensure their safety. For over a century, researchers have been discussing reinforced concrete (RC) members lacking shear reinforcement for their shear capacity. The maximum load located on RC slab bridges has been estimated using plasticity-based techniques. However, the drawback of these techniques is that the calculations need to be customized for the specific geometry of the bridge. Also, despite being quite time-consuming, nonlinear finite element (NLFE) models in combination with suitable safety formats help assess RC slab bridges. Despite the need to evaluate a great deal of bridges, computationally efficient approaches should be applied. FE models can be adopted to determine bending moments and shear stresses caused by applied load combinations. Usually, for RC beams, the traditional flexural theory can be used to estimate the bending moment capacity. Also, ANNs is a useful numerical method to predict the shear capacity of RC slabs. This method uses machine learning (ML) to more accurately analyze and predict the behavior of structures under different conditions. This model can also be adopted to assess the safety and performance of RC slab bridges, thereby improving the design and implementation of civil projects. In general, the shear capacity of one-way slabs can be determined based on Eqs. 1 and 2 [7]. In these equations, ρ_w represents the percentage of longitudinal tensile reinforcement, λ is the coefficient for considering the effect of lightweight concrete, f'c is the compressive strength of concrete, N_u is the factored axial force, A_g is the cross-sectional area, b_w is the cross-sectional width, and d is the effective depth of the slab.

$$V_c = (0.17\lambda\sqrt{f_c'} + \frac{N_u}{6A_g})b_w\, d \tag{1}$$

$$V_c = (0.66\lambda\rho_w^{\frac{1}{3}}\sqrt{f_c'} + \frac{N_u}{6A_g})b_w\, d \tag{2}$$

Shen et al. [1] evaluated the performance of ML models for estimating FRP-RC slabs' punching shear strength (PSS). They compared models in terms of performance using ML algorithms, including ANNs and Support Vector Machine (SVM). Furthermore, the predicted accuracy was checked by experimental models and design codes. The comparative results showed that adaptive boosting produced the highest predicted precision. The predicted process was then illustrated using Shapley Additive Explanation (SHAP). Lantsoght et al [2] evaluated the performance of an extended strip model (ESM) used for slabs subject to different combinations of loads. In addition to accurate estimation of the maximum concentrated load located on the slabs, the ESM can be employed to evaluate current bridges that are subject to heavy truck loads. In fact, the slab behavior was evaluated under a load combination. For this purpose, eight slabs, with the same dimensions of 5m*2.5m*0.3m, were tested. A total of 23 experiments were conducted on the slabs, with 2 or 4 tests on each slab based on loading configuration. RC slab bridges were assessed using the following load combinations: concentrated/distributed live loads, superimposed dead load, and self-weight.

For these experiments, a more straightforward loading scheme was utilized, including a single near-support concentrated load with a line load that is applied to the entire width of the slab. The maximum line load and slab failure time were then determined. According to the basic assumption, a slab under a line load showed the same behavior as a beam under a concentrated load. Nevertheless, during the preparation of these experiments, it was unknown how a slab under a concentrated load and a line load would exactly behave the same [3, 4]. Hoang et al. [5] employed sequential piecewise multiple linear regression (SPMLR) and ANNs to estimate SFRC slabs' PSC.

This study aimed to enhance practical design equations' accuracy by applying ML. The structure of the PMLR model was automatically constructed through the implementation of a sequential algorithm. In addition, ANN-based prediction models were trained by algorithms of Levenberg-Marquardt (LM) backpropagation and gradient descent.

According to the experimental results, structural engineers may find the SPMLR model a promising tool in supporting them during the design stage of structures that incorporate SFRC flat slabs, as it provided prediction results for both ANNs and practical design equations. Alkroosh et al. [6] sought to model RC flat slabs' punching shear by reviewing soft computing and predict it by utilizing gene expression programming (GEP).

The GEP model was designed according to case histories, including the PSS. Two datasets were employed: a training dataset and a validation dataset. According to the results, the GEP model outperformed traditional approaches in accurately modeling the intricate relationship between punching shear and the factors influencing it and also in predicting the PSS. The GEP model's performance was further evaluated by comparing its predictions with those of three currently used methods, namely BS-8110, CEP-FIP MC, and ACI-318 [7-9]. Aggarwal et al. [10] adopted data mining techniques for PSC estimation of concrete slabs to enhance the predicted accuracy of punching loads. The punching load of RC slab–column connections was modeled and estimated using different data mining techniques: ANNs, Generalized Neural Networks (GRNNs), and Adaptive Neuro-Fuzzy Inference System (ANFIS).

They analyzed the existing dataset, demonstrating the superiority of the ANFIS model over other models in determining the coefficient of correlation (Cc). In addition, the effective slab depth (d) was shown to be the most influencing parameter in punching load estimation of RC slab column connections.

Elshafey et al. [11] employed neural networks to predict the PSS of two-way slabs.

They explored the connection between slab characteristics and shear strength by analyzing available experimental data and introduced new equations to estimate the PSS, which were a good match with experimental data. According to this research, since neural networks can yield results that closely resemble experimental data, the proposed equations are reliable.

As mathematical tools, ANNs (usually comprising a single input layer, a single output layer, and one or more hidden layers) are intended for imitating the function of biological neurons in human brain and ascertaining a functional relation between input-output data that have been measured, which is typically superior to that found by regression methods [12]. Shu et al. [13] investigated some RC bridge deck slabs for their shear capacity, especially without shear reinforcement.

The punching shear problems in these slabs, especially subjected to concentrated loading, were also discussed.
To this aim, a multi-level evaluation strategy was applied in order to a real-life RC bridge deck slabs (age: 55 years old) using full-scale field experiment. The mentioned strategy offers the science of engineers a well-defined scheme for exploiting enhanced techniques of structural analysis. The distinctions between the methods for analyzing punching and one-way shear behavior of slabs were discussed based on certain parameters, e.g., concentrated load location, distribution of shear force, and boundary conditions. Belletti et al. [14] performed NLFE analyses on RC slabs. Numerical and analytical procedures can be used to evaluate RC structures' shear resistance. NLFE analyses belong to IV-level approximation (the highest level) because they carefully examine real material properties and hidden structural capacities. They used the NLFE analyses to re-evaluating the carrying capacity of existing bridges and viaducts.
For this purpose, several experimental results were compared with analytical and numerical results. Lantsoght et al. [15] investigated one-way slab shear under near-support concentrated loads. These slabs are designed typically for shear by setting the beam and punching shear resistance over an effective width. However, relevant test data are currently limited.
One-way slabs underwent a set of experiments to assess their shear strength. According to the results, slabs exhibited different shear behavior than beams. Liu and Guo [16] investigated the vertical shear capacity of ultra-high-performance concrete (UHPC) slabs with steel reinforcement in a cantilevered state. The results of their study showed that the use of high-strength concrete increased the shear capacity of the slab by 69.97% compared to the ordinary concrete. In 2024, Truong et al. [17] predicted the punched shear capacity of concrete slabs using a nature-inspired metaheuristic algorithm. The results of the study indicate the appropriate performance of that algorithm to determine the shear capacity of concrete slabs. Cao et al. [18] investigated the shear stress transfer behavior in composite concrete slabs with lattice beam. The results showed that the load-bearing capacity of polished surfaces was 26.5% lower than that of rough surfaces, and they emphasized that the angle of shear reinforcement should not exceed 90 degrees.
Shirkhani et al. [19] predicted of bond strength between concrete and rebar under corrosion using ANN. In 2025, Nouri et al. [20] predicted of axial compression capacity of GFRP-reinforced concrete column using soft computing methods. Chen et al. [21] using ANN, GEP and MLR presented a predictive model for recycled aggregate concrete filled circular steel tube columns. In 2024, Fakharian et al. [22] studied bond strength prediction of externally bonded reinforcement on groove method (EBROG) using MARS-POA. Shabani Ammari et al. [23] investigated flexural strengthening of corroded steel beams with CFRP by using the end anchorage with machine learning methods. In 2025, Chen et al. [24] optimizing compressive strength prediction in eco-friendly recycled concrete via artificial intelligence models. Nouri et al. [25] presented an integrated optimization and ANOVA approach for reinforcing concrete beams with glass fiber polymer.
The large volume of studies conducted on the use of artificial intelligence capabilities in solving various construction problems indicates the importance of this study.
In this study, after modeling five one-way slab samples with different ratio (length to width) higher than 2 by ETABS, the nominal shear strength response of the concrete slab was recorded for different positions of concentrated load, and then used to train the neural network. After checking the accuracy of the neural network in correctly predicting of the shear strength, relations were presented using nonlinear regression to determine the shear capacity of one-way slabs.
After that, the structure of the optimal neural network has been described and the predicted results by the neural network were determined.
Finally, the relationships obtained for predicting the shear capacity of a one-way slab have been showed in details.

2. Introduction to neural networks

A neural network is a massively parallel processor that consists of simple processing units, and its most important advantage over other intelligent systems is the network's ability to learn from the environment and increase efficiency during training. Figure (1-a) shows a model of a node that is the basic processing unit of a neural network and its mathematical model.
X_{ij} is the input values of node j, W_{ij} is the network weights, f is the excitation function, b_j is the bias value, and O_j is the output of node j.
In general, a neural network consists of 5 different parts, which include inputs, weights, bias, performance function, and output. Inputs are the information entered to the network, weights show the influence of the input on the output, and bias is the amount of influence of the input of a fixed value of 1 on the neuron. Weights and bias are adjustable and the performance function is also chosen by the designer.
In general, neural networks have three types of input layers, hidden layers, and output layers.
The general structure of the neural network is shown in Figure (1-b).

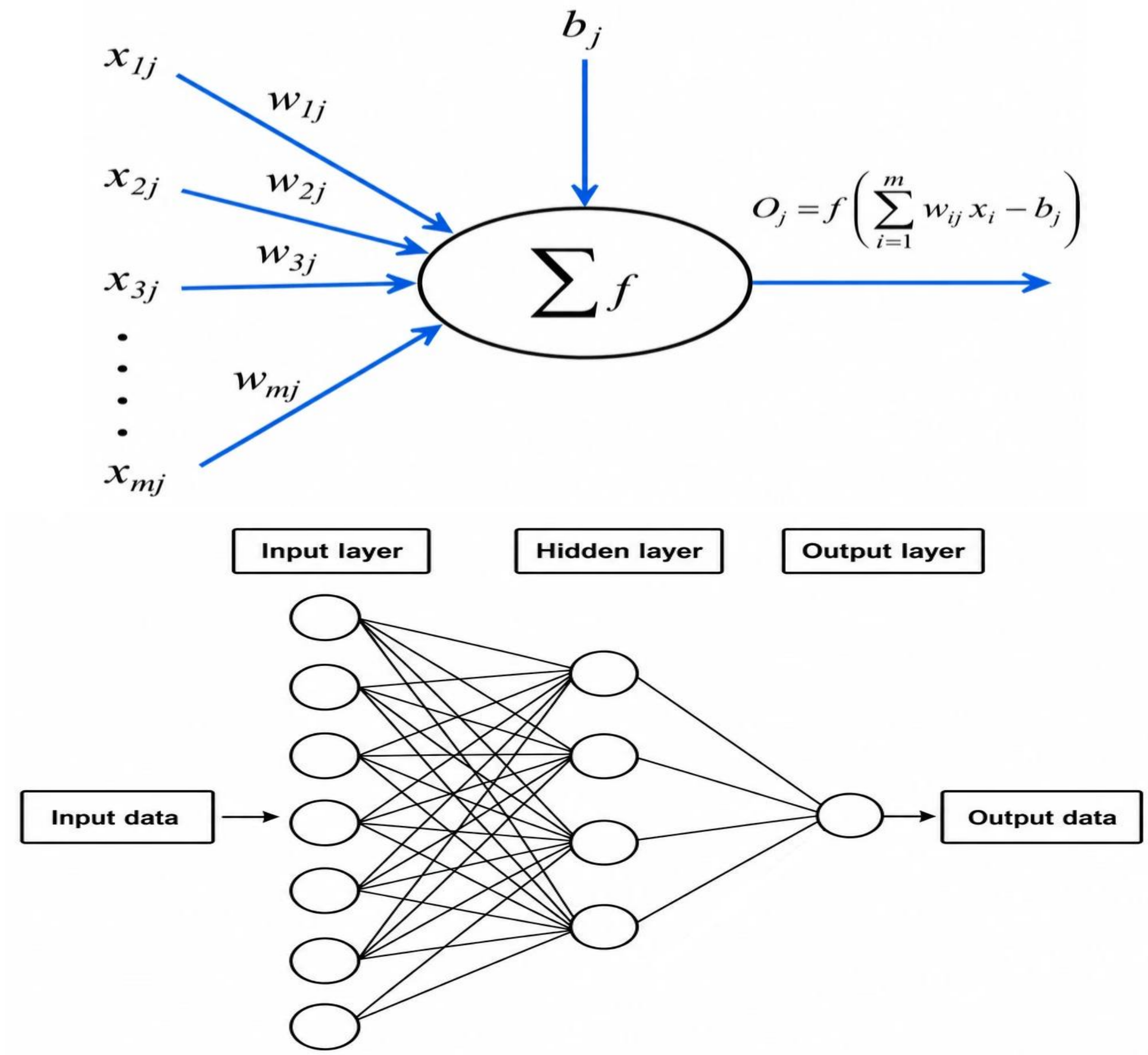

Figure1. Performance and structure of the neural network

3. Regression analysis

Many natural phenomena contain directly or indirectly linked variables. A variable depends on some other effective variables, whose relationship is not governed by any specific physical law. This law can somehow be estimated by various prediction methods, including regression analysis. Regression analysis is a statistical method to calculate and find the relationships between one dependent variable and one or more independent variable. This method gives us insights into changes in a dependent variable when each independent variable changes while other dependent variables remain constant. In most cases, it is employed to compute a function of independent variables to predict the dependent variable. Nowadays, regression analysis is extensively used for prediction. It is performed in various ways, including linear regression and least squares regression (LSR), as the most popular ones. As a type of regression analysis, linear regression reflects the relationships between a dependent/independent variable or more modeled by using linear regression equations. However, in general, nonlinear regression aims to discover a proper nonlinear equation for the purpose of the aforementioned relationship. Although the first type of regression, LSR can be traced back to Gauss (1834) and Legendre (1835), the term "regression" was coined by Francis Galton (1488) in his paper on regression toward the mean. Regression methods have been employed by various studies to date. Especially, regression analysis has been applied successfully in recent decades for predicting concrete properties [2, 15, 16, 17].

4. Numerical examples

4.1. Modeling one-way slabs

One-way slab is supported in only one direction or the supports are significantly stiffer in one direction than the other. The span length-to-width ratio in one-way slabs is often greater than 2. Thus, in this study five concrete slabs with length-to-width ratios of 2, 2.22, 2.5, 2.85, and 3.33 has been modelled by ETABS. The middle (centre) of the shorter span (Lx) was then subjected to a concentrated load, and different positions of the longer span (Ly), and shear strength responses of slabs were then recorded. The concentrated load positions were applied to the slab at intervals of 0, 0.1, 0.2, 0.3, 0.4, 0.5, 0.6, 0.7, 0.8, 0.9, and 1 times the Ly. Table 1 lists the geometric characteristics of the five initial slabs modelled by ETABS. Notably, the minimum slab thickness was assumed to be L/20 in different modes. Herein, the long slab length was considered to be constant (i.e., 10 m) and its width and thickness as variable. The compressive strength of the concrete considered as 25MPa. Furthermore, the thickness of the slab considered as a variable. Besides, 35 cm-thick shear walls were utilized to provide support. Concentrated loading consisted of a 15kN live load. Figure 2 illustrates a 3D schematic slab modelled by ETABS.

Table 1. Geometric characteristics of the slabs

Sample	Aspect ratio (L_1/L_2)	L_1 (mm)	L_2 (mm)	Slab thickness t (mm)
1	2	10000	5000	250
2	2.22	10000	4500	225
3	2.5	10000	4000	200
4	2.85	10000	3500	175
5	3.33	10000	3000	150

Note that concentrated load was applied for ten different positions along the Ly in the middle of the short slab span.

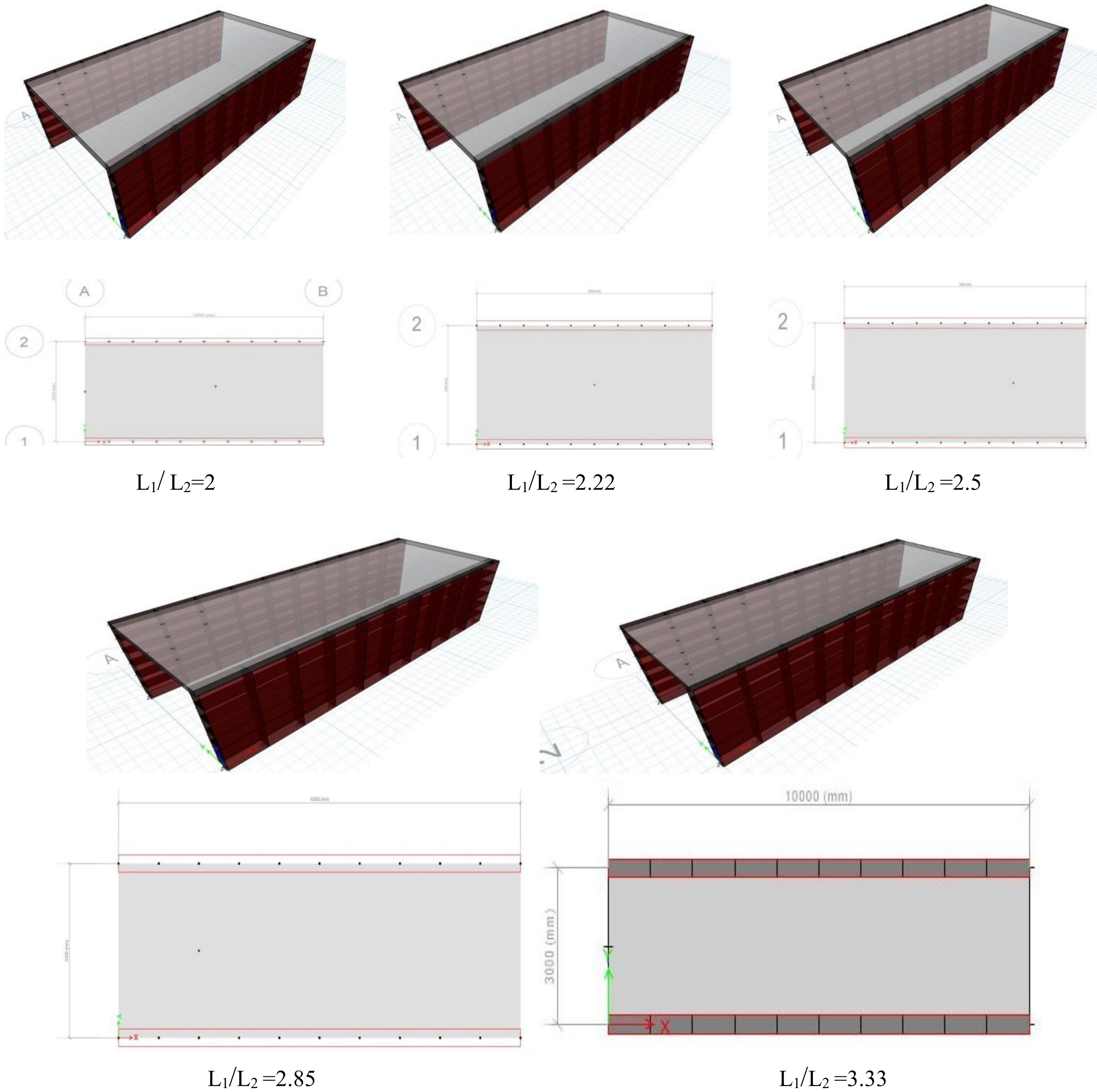

Figure 2. A 3D schematic diagram of the slabs modeled in ETABS

10.57647/Jsm.2025.1704.17

4.2. Result of Analysis of one-way slabs

After modelling of 55 different slabs, including 5 one-way slabs with 11 different concentrated load application positions, shear capacity responses of slabs were captured from the Shell Force Stress--V23 menu with a strength-reduction factor of 0.75. It should be noted that the geometry of the one-way slab and the location of the concentrated loads imposed a limitation on the number of models to 55 initial models. Although this limited number cannot be the basis for definitive conclusions about the code relationships. However, the main goal of this study is not to question the code relationships, but rather to demonstrate the capability of the neural network method as an ideal tool for predicting the shear capacity of concrete slabs.

To control the results, the maximum deflection obtained from the software models was compared with the maximum allowable deflection. The results indicated that the one-way slab deflection did not exceed the permissible value (i.e., L/480) in any of the simulated models. Figure 3 shows the shear stress distribution for selected models. Note that the slab control direction analysis was performed based on the combination of service loads. Table 2 presents the numerical values for concrete slabs' shear capacity for different modelling styles as well as slab deflection vs. maximum allowable deflection values. These numerical values were employed as primary data for training the neural network.

Notably, the nominal shear capacity of the slabs was estimated by dividing the shear capacity received from the software by 0.75.

The primary reason for adopting a linear formulation in this study was to focus on developing an ANN-based predictive framework that relies on simplified input–output relationships without introducing additional complexities from nonlinear FEM simulations. Nonlinear modelling (including cracking, reinforcement slip, and post-yielding effects) indeed provides deeper insight into structural behavior; however, it requires extensive experimental calibration and significantly larger datasets. In our simplified model, explicit cracking and reinforcement flow were not directly modelled, because our dataset was limited and derived from idealized slab configurations.

However, the ANN predictions indirectly capture some of these effects since the training data reflect the global shear response under concentrated loading.

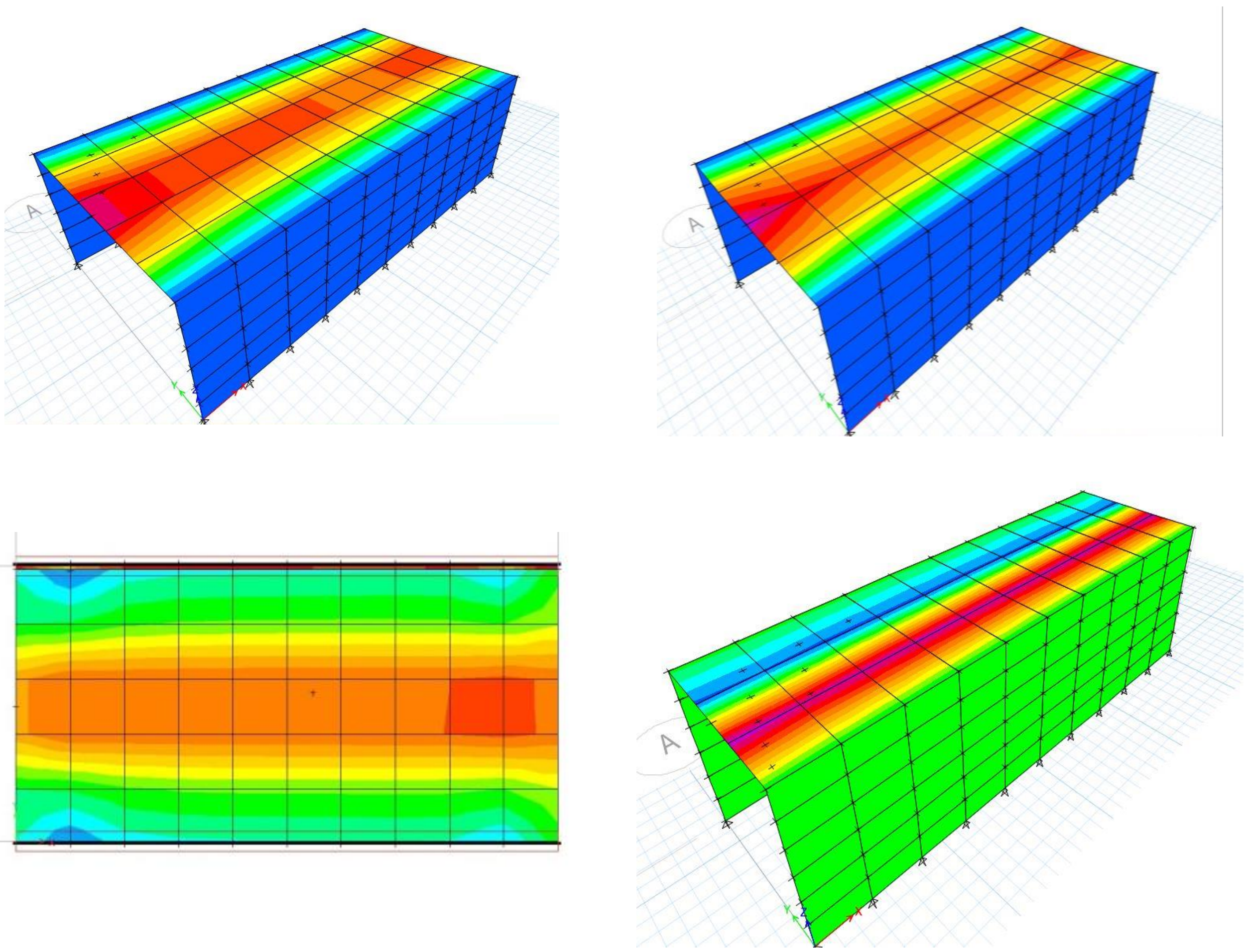

Figure 3. Shear stress distribution for selected slabs

10.57647/Jsm.2025.1704.17

Table 2. Numerical values for the shear capacity of the slabs for different modeling styles

Sample	Aspect ratio (L1/L2)	Load application point x/L_1	Nominal shear capacity of concrete (kN)	Slab deflection (mm)	[Maximum] allowable deflection ($L_2/480$)
1	2	0	53.3	4.04	10.42
2	2	0.1	52.9	3.184	10.42
3	2	0.2	52.56	3.46	10.42
4	2	0.3	51.24	3.39	10.42
5	2	0.4	50.37	3.39	10.42
6	2	0.5	50.02	3.39	10.42
7	2	0.6	50.4	3.39	10.42
8	2	0.7	51.244	3.39	10.42
9	2	0.8	52.56	3.46	10.42
10	2	0.9	52.95	3.604	10.42
11	2	1	53.43	4.046	10.42
12	2.22	0	47.15	3.455	9.375
13	2.22	0.1	46.39	3.144	9.375
14	2.22	0.2	46.27	2.965	9.375
15	2.22	0.3	44.67	2.875	9.375
16	2.22	0.4	43.7	2.834	9.375
17	2.22	0.5	43.38	2.817	9.375
18	2.22	0.6	43.83	2.834	9.375
19	2.22	0.7	44.7	2.875	9.375
20	2.22	0.8	46.27	2.965	9.375
21	2.22	0.9	46.39	3.14	9.375
22	2.22	1	47.15	3.455	9.375
23	2.5	0	43.27	1.97	8.33
24	2.5	0.1	42.37	1.64	8.33
25	2.5	0.2	41.93	1.51	8.33
26	2.5	0.3	39.89	1.5	8.33
27	2.5	0.4	39.89	1.5	8.33
28	2.5	0.5	39.77	1.51	8.33
29	2.5	0.6	39.89	1.5	8.33
30	2.5	0.7	39.89	1.5	8.33
31	2.5	0.8	41.93	1.51	8.33
32	2.5	0.9	42.37	1.64	8.33
33	2.5	1	43.27	1.97	8.33
34	2.85	0	40.42	2.16	7.29
35	2.85	0.1	37.56	1.72	7.29
36	2.85	0.2	36.02	1.67	7.29
37	2.85	0.3	35.9	1.66	7.29
38	2.85	0.4	35.9	1.67	7.29
39	2.85	0.5	35.86	1.67	7.29
40	2.85	0.6	35.9	1.67	7.29
41	2.85	0.7	35.91	1.67	7.29
42	2.85	0.8	36.01	1.67	7.29
43	2.85	0.9	37.56	1.72	7.29
44	2.85	1	40.42	2.16	7.29
45	3.33	0	52.8	1.91	6.25
46	3.33	0.1	52.94	1.55	6.25
47	3.33	0.2	49.9	1.51	6.25
48	3.33	0.3	49.79	1.5	6.25
49	3.33	0.4	49.71	1.49	6.25
50	3.33	0.5	49.63	1.49	6.25
51	3.33	0.6	49.71	1.49	6.25
52	3.33	0.7	49.79	1.5	6.25
53	3.33	0.8	49.9	1.5	6.25
54	3.33	0.9	52.94	1.55	6.25
55	3.33	1	52.8	1.9	6.25

10.57647/Jsm.2025.1704.17

4.3. ANN-based formulation for predicting the one-way slabs' shear capacity

Due to the current limitations, many experimental or software samples (prototypes) cannot be studied to obtain a general relation. This weakness can be overcome by exploiting neural network capabilities as a prominent subset of AI. As previously mentioned, this study utilizes the data listed in Table 2 to train the neural network. The load application point was defined as the neural network input and concrete shear strength as its output or target for five different one-way slab models. Next, the neural network learned the logical relationship between inputs and outputs. For this purpose, data were divided into three sets, i.e., testing (15%), training (70%), and validation (15%). Hence, shear capacity prediction of slabs could be carried out for different positions for applying the concentrated load along the long slab span. Table 3 summarizes the efforts made to attain the most optimum neural network topology. The findings imply that using 20 neurons in each hidden layer and two intermediate layers yields the most optimum neural network topology. Figure 4 depicts the linear regression for the training, testing, and also validation functions in various modes to determine the most optimum neural network topology. Moreover, Table 3 compares control criteria numerically to find the most optimum neural network out of the 12 studied modes. The first control criterion was regression numerical values. Regression values<0.9 indicated unacceptable results (here, Modes 4, 6, 7, 10, 9, and 11, which were excluded from the first control list of all potential neural networks). It is noteworthy that the next control criterion was the performance numerical value. Lower performance numerical values indicated more optimal results (here, Modes 1, 8, and 12 were excluded from the same list of because of their high performance numerical values). Based on the last control criterion, the higher correlation between linear regression for the training, testing, and validation functions indicated better results (here, Mode 3 showed the strongest correlation among modes 2, 3, and 5). Consequently, the most optimum neural network was a double-layer network with 10 neurons in each layer. In nomination, while the first number after Ffb denotes the number of layers, the second one indicates the number of neurons per layer. For instance, Ffb310 represents a neural network characterized by 3 hidden layers, each of which contains 10 neurons.

Table 3. Applied parameters to determine the most optimum neural network topology

Sample	Model acronym	Perfor(10^{-9})	Mu(10^{-10})	Gradient	Reg
1	Ffb110	2352	100	0.00149	0.93
2	Ffb120	4.18	0.00001	0.000111	0.96
3	Ffb210	59.6	1	0.000188	0.98
4	Ffb220	5590000	10000	0.00044	0.79
5	Ffb230	0.349	0.00001	0.000271	0.94
6	Ffb310	2152	10	0.00169	0.85
7	Ffb320	6110000	1000000	0.103	0.80
8	Ffb330	1038	1	0.00247	0.97
9	Ffb410	194800	100000	0.00146	0.63
10	Ffb420	3510	1	0.00341	0.89
11	Ffb430	14900000	1000	0.00179	0.71
12	Ffb510	108	1000	0.000747	0.96

Shear capacity prediction of concrete was conducted for the five models after obtaining the most optimum neural network topology. To this aim, concrete slabs' load-bearing capacity was predicted for applying the concentrated load along the slab Ly at distances of 100, 200, 300, 9700, 9800, 9900, and 10000 mm from the corner of the slab (101 different loading position). Afterward, the shear capacity predicted by the neural network for the five studied concrete slabs was compared with the real amounts. Figure 5 displays the linear regression for the training, testing, and validation functions of the neural network utilized to predict the shear capacity of one-way concrete slabs (dimension ratio [Ly/Lx]: 2). As mentioned earlier, the closer the linear correlation coefficient of the data (i.e., regression) is to 1, the neural network predicts the desired parameter (i.e., shear strength of one-way slabs [dimension ratio: 2]) with higher accuracy. The neural network obtained 0.998%, 0.994%, and 0.977% accuracy, in predicting the above parameter, in the phases of training, validation, and testing, respectively, and 0.994% accuracy in general. This indicated that the neural network could predict the one-way slabs' (dimension ratio: 2) shear capacity precisely. Table 4 shows the numerical values of regression for predicting the shear strength of one-way slabs in the training, evaluation and testing stages.

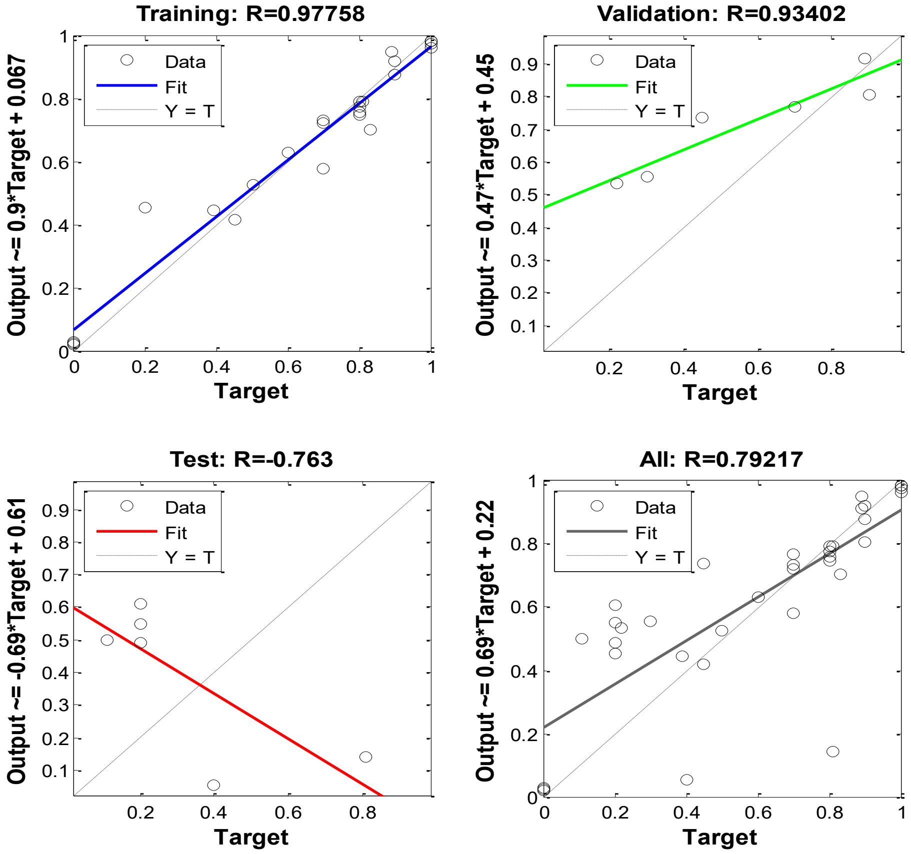

(1)

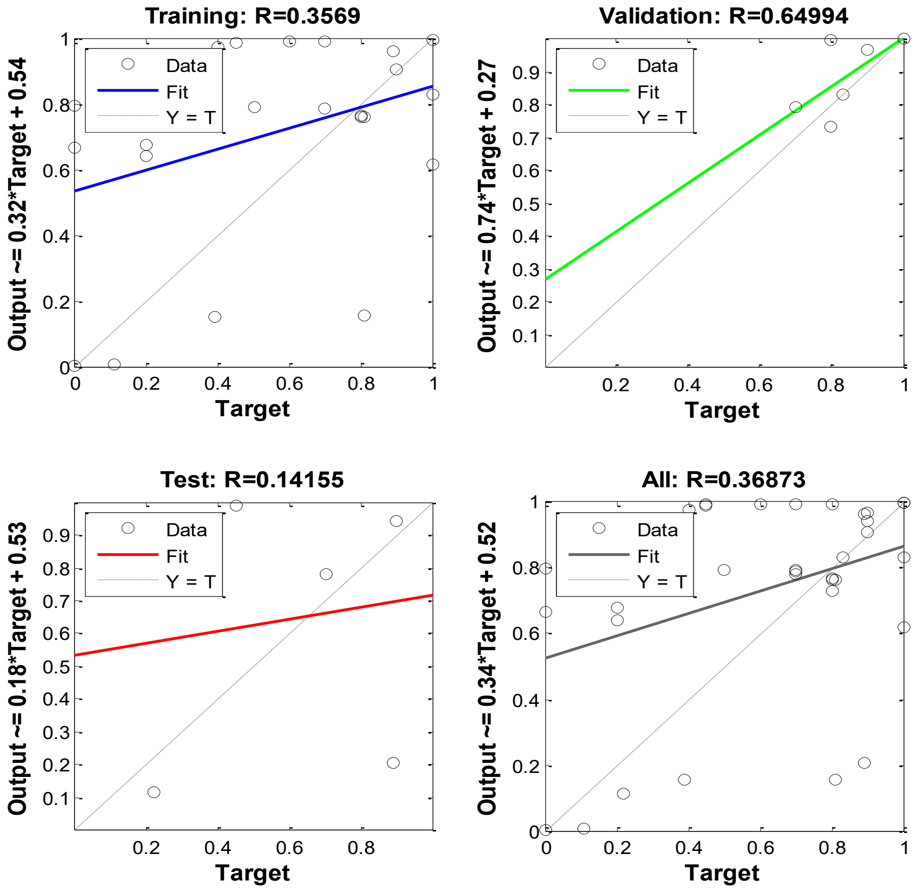

(2)

10.57647/Jsm.2025.1704.17

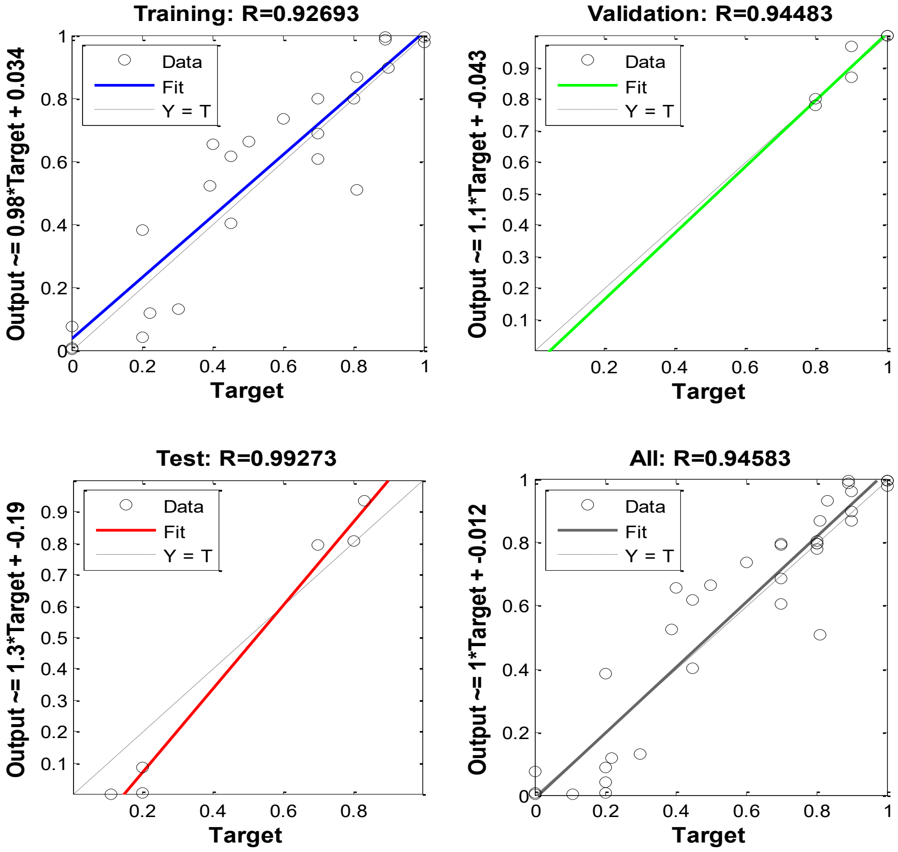

(3)

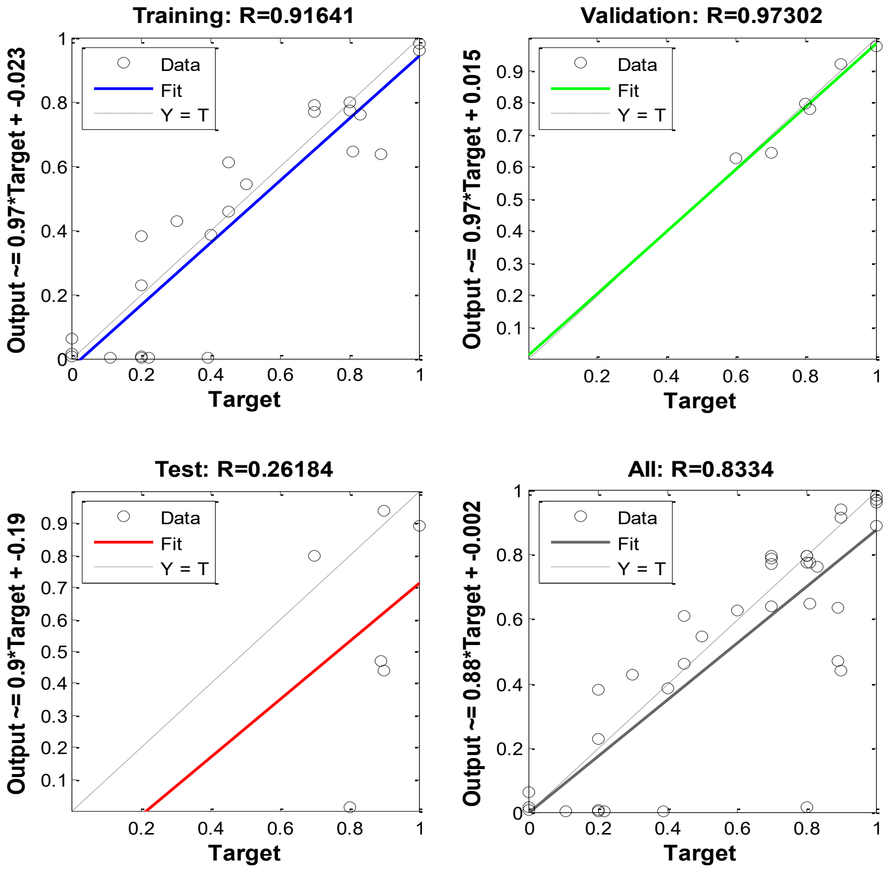

(4)

10.57647/Jsm.2025.1704.17

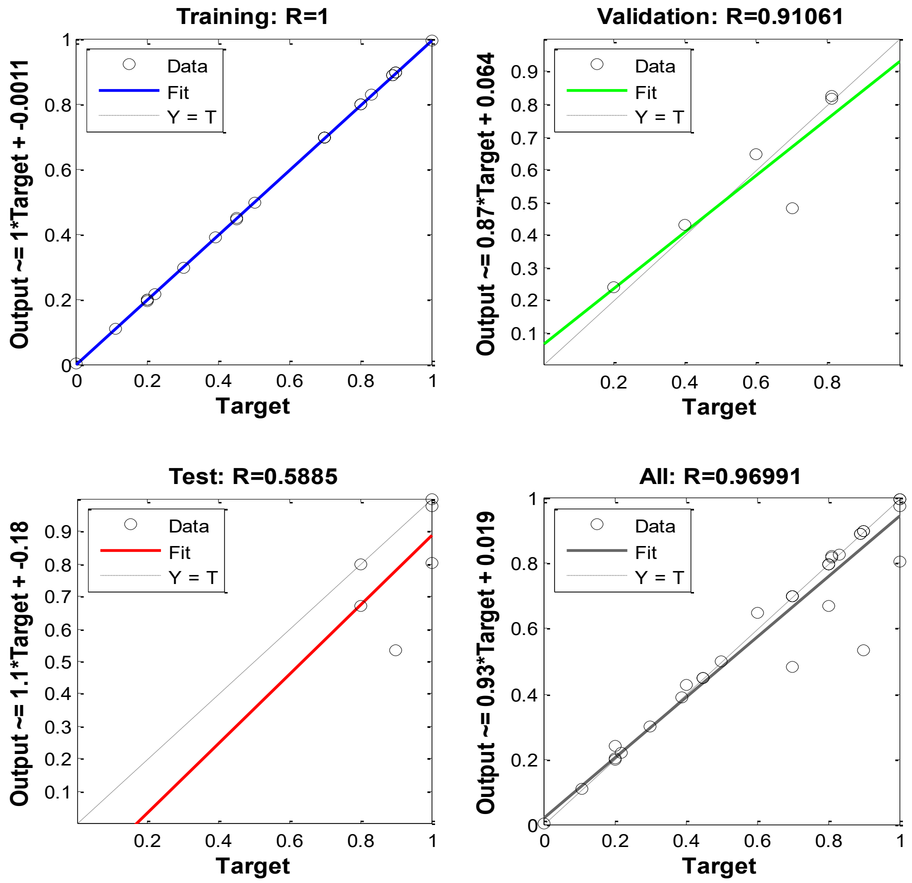

(5)

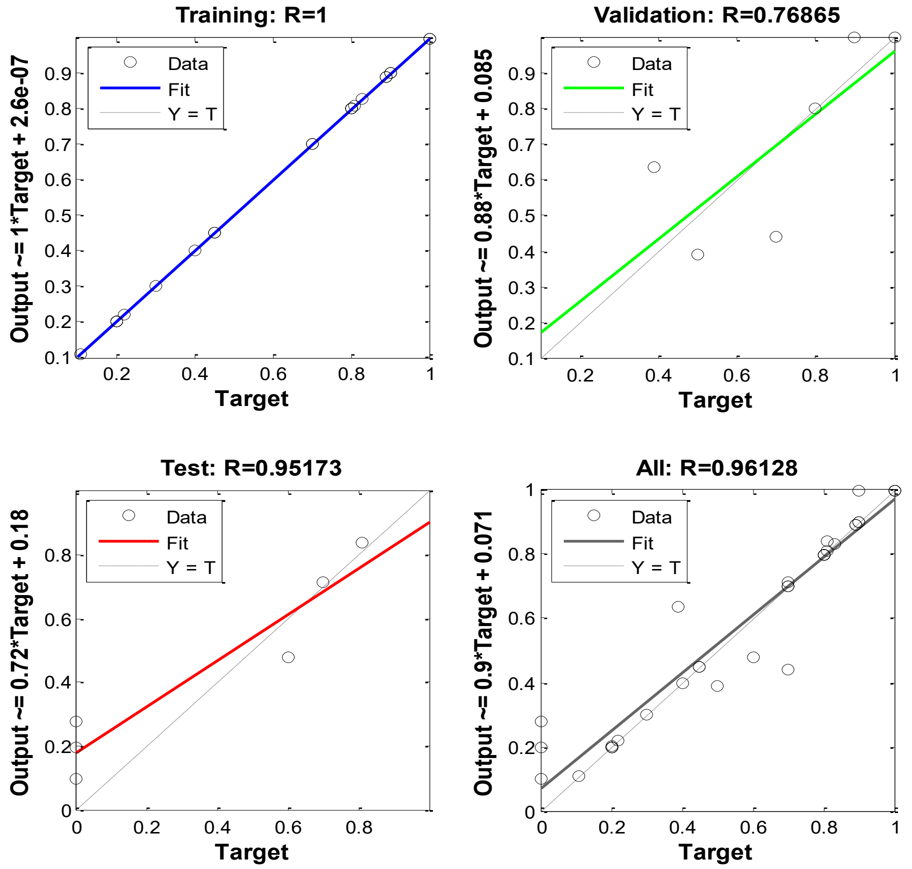

(6)

10.57647/Jsm.2025.1704.17

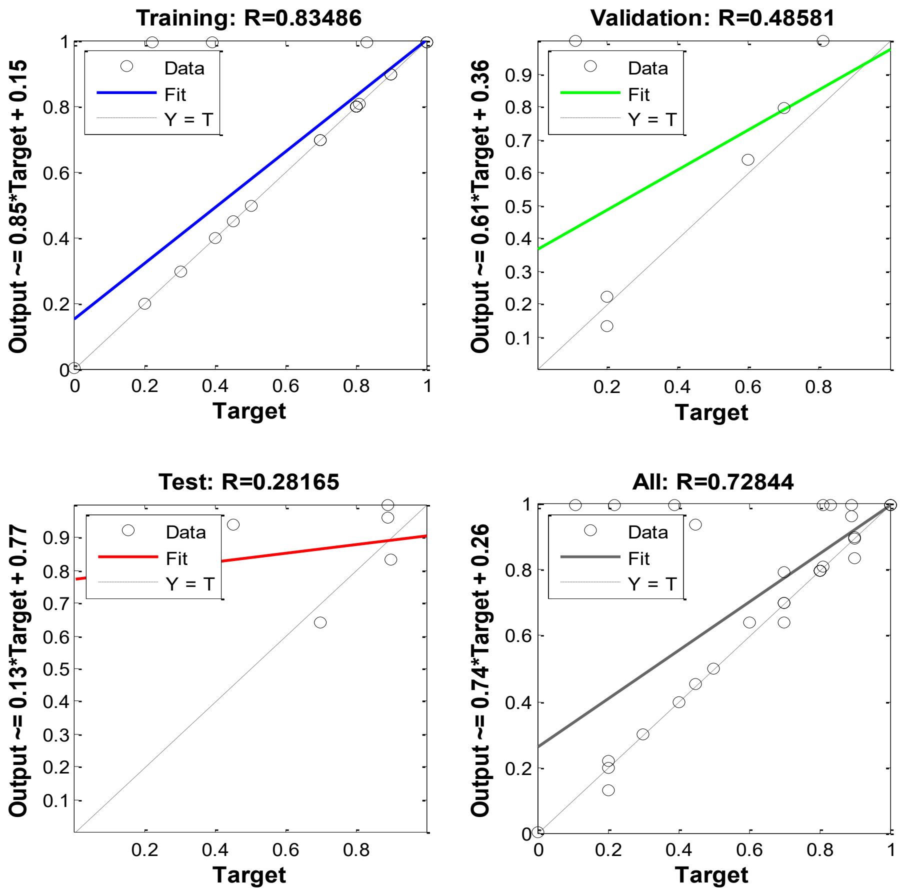

(7)

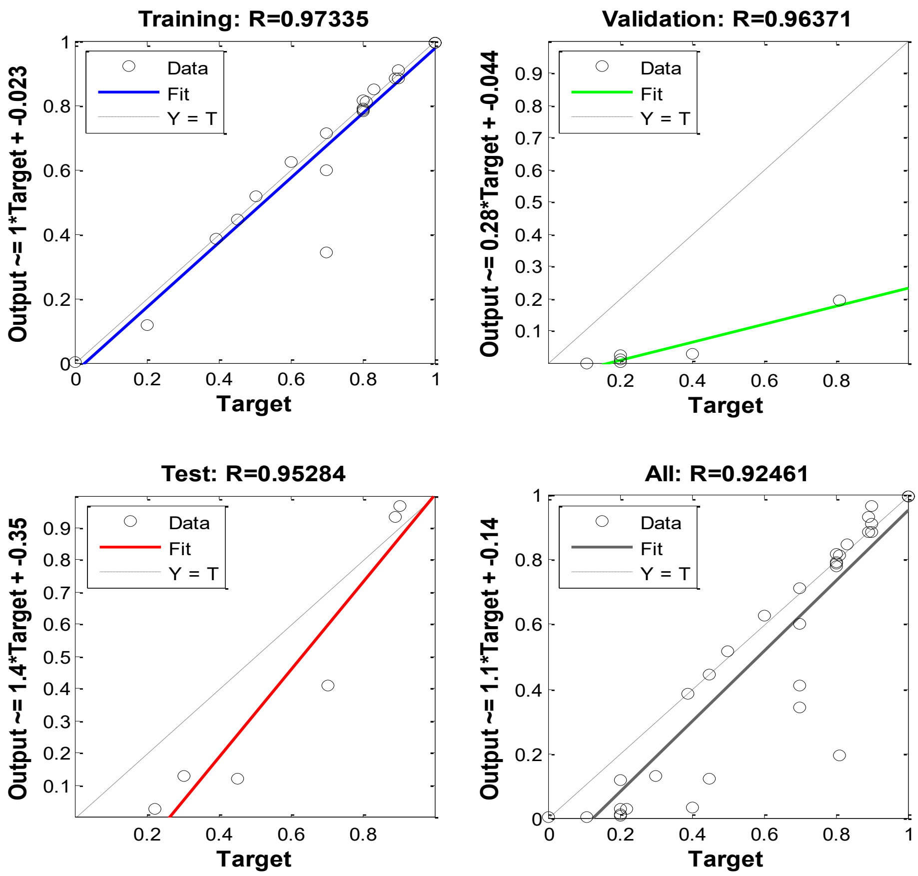

(8)

10.57647/Jsm.2025.1704.17

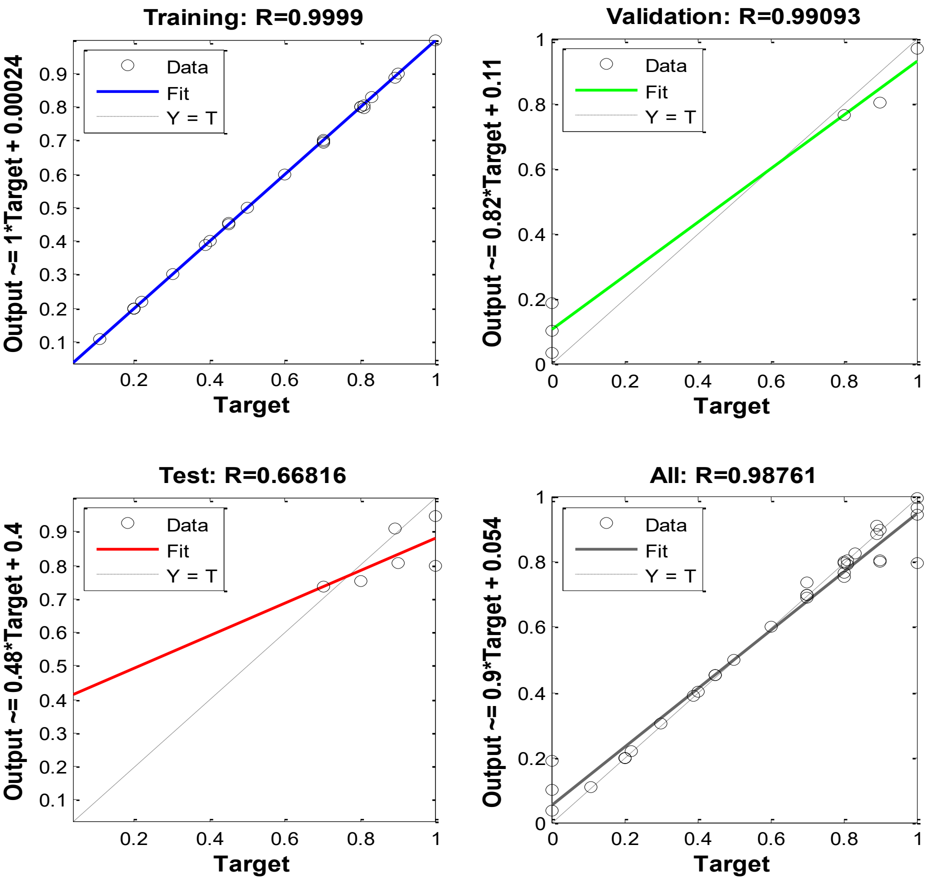

Training: R=0.9999
Output ~= 1*Target + 0.00024
Validation: R=0.99093
Output ~= 0.82*Target + 0.11
Test: R=0.66816
Output ~= 0.48*Target + 0.4
All: R=0.98761
Output ~= 0.9*Target + 0.054
Data
Fit
Y = T
Target

(9)

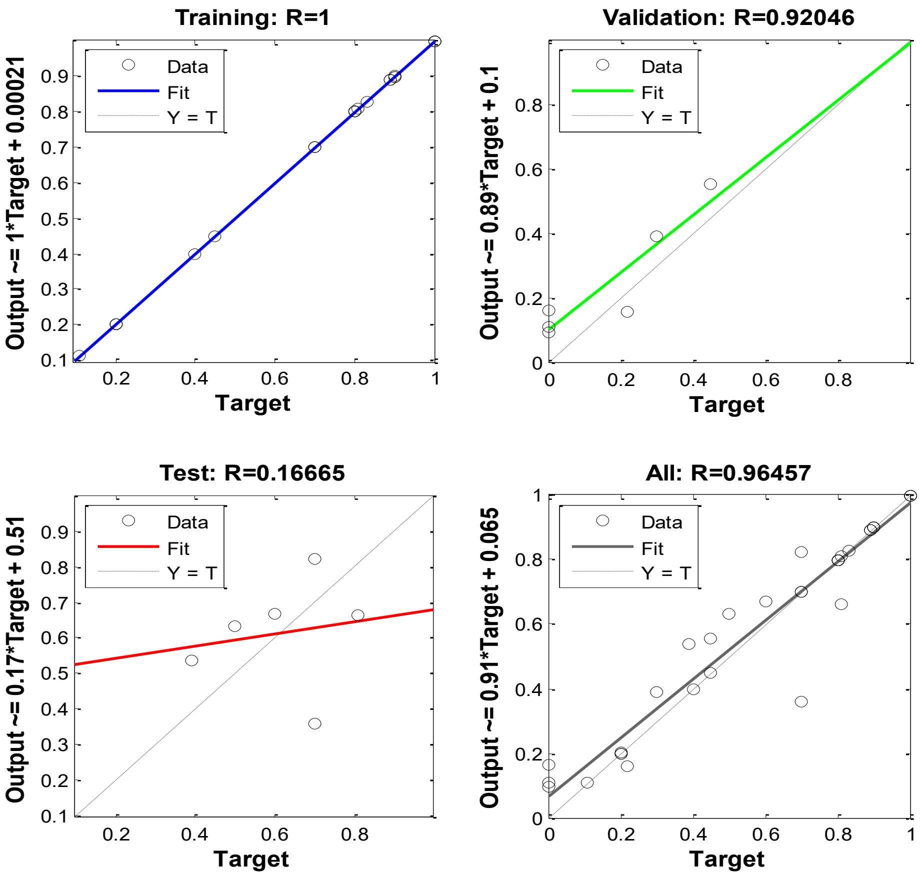

Training: R=1
Output ~= 1*Target + 0.00021
Validation: R=0.92046
Output ~= 0.89*Target + 0.1
Test: R=0.16665
Output ~= 0.17*Target + 0.51
All: R=0.96457
Output ~= 0.91*Target + 0.065
Data
Fit
Y = T
Target

(10)

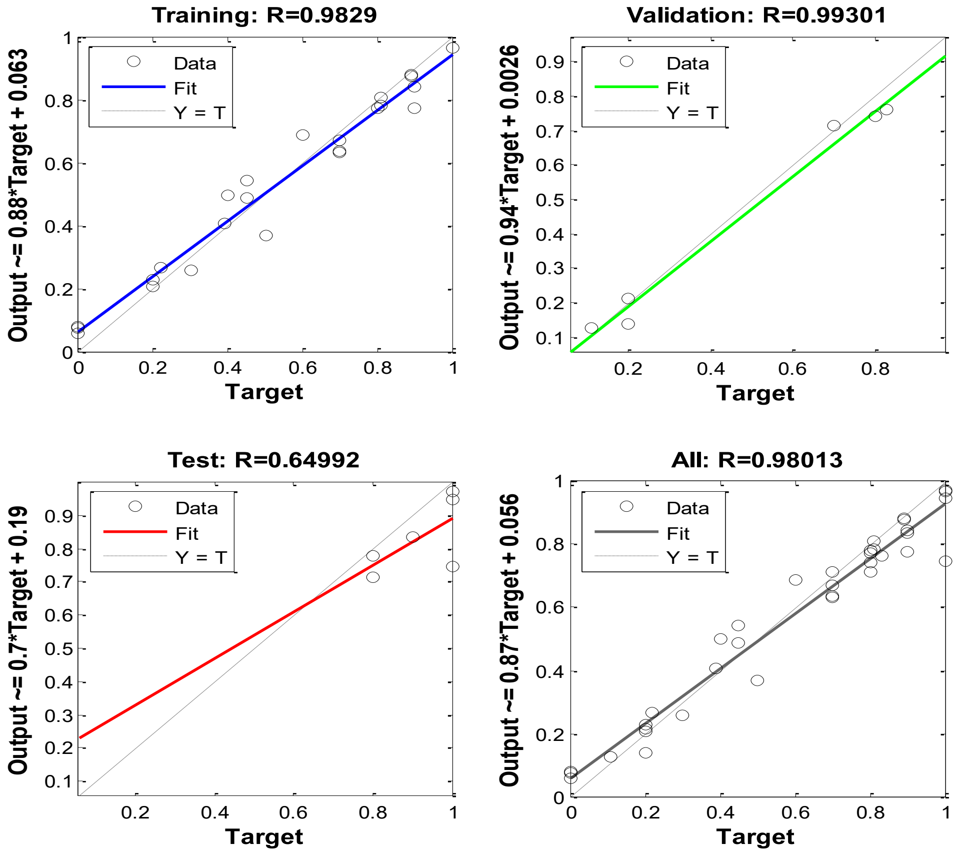

(11)

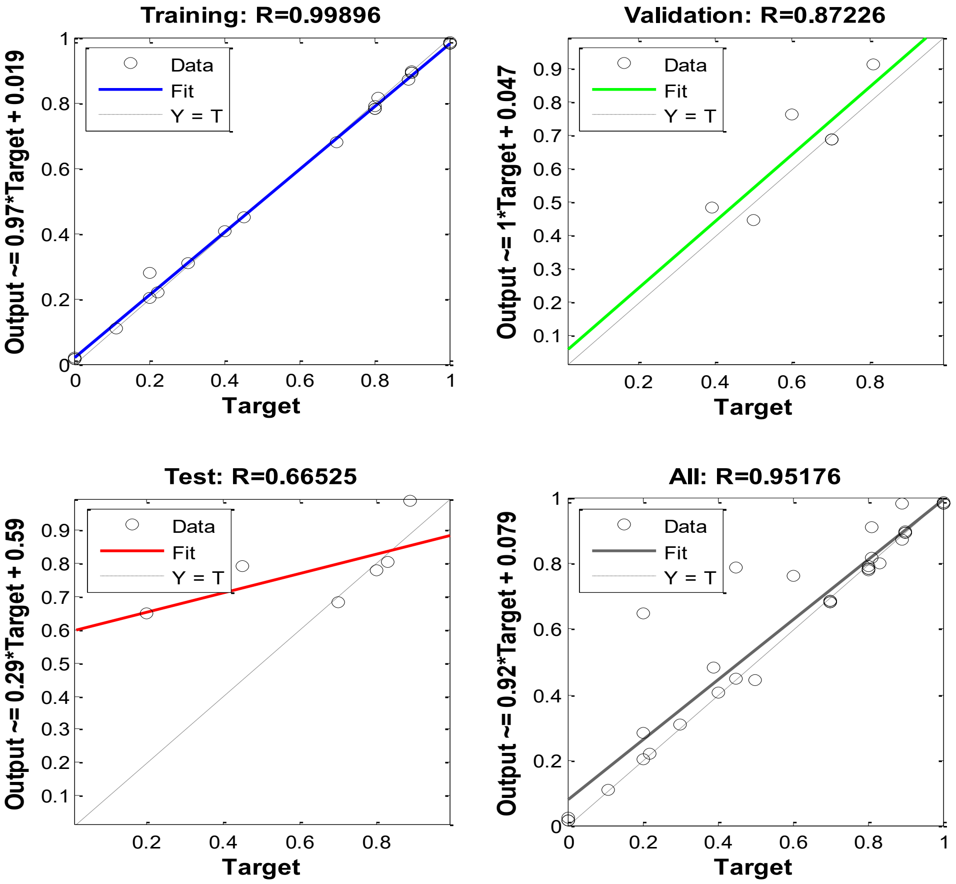

(12)

Figure 4. Linear regression for the training, testing, and validation functions for various modes of neural networks

Table 4. Numerical values of regression in training, evaluation and testing modes for predicting the shear strength of one-way slabs

L_1/L_2	Training	Validation	Test	All
2	0.998	0.994	0.977	0.994
2.22	0.987	0.995	0.996	0.99
2.5	0.99	0.97	0.992	0.988
2.85	0.94	0.919	0.940	0.936
3.33	0.994	0.926	0.994	0.987

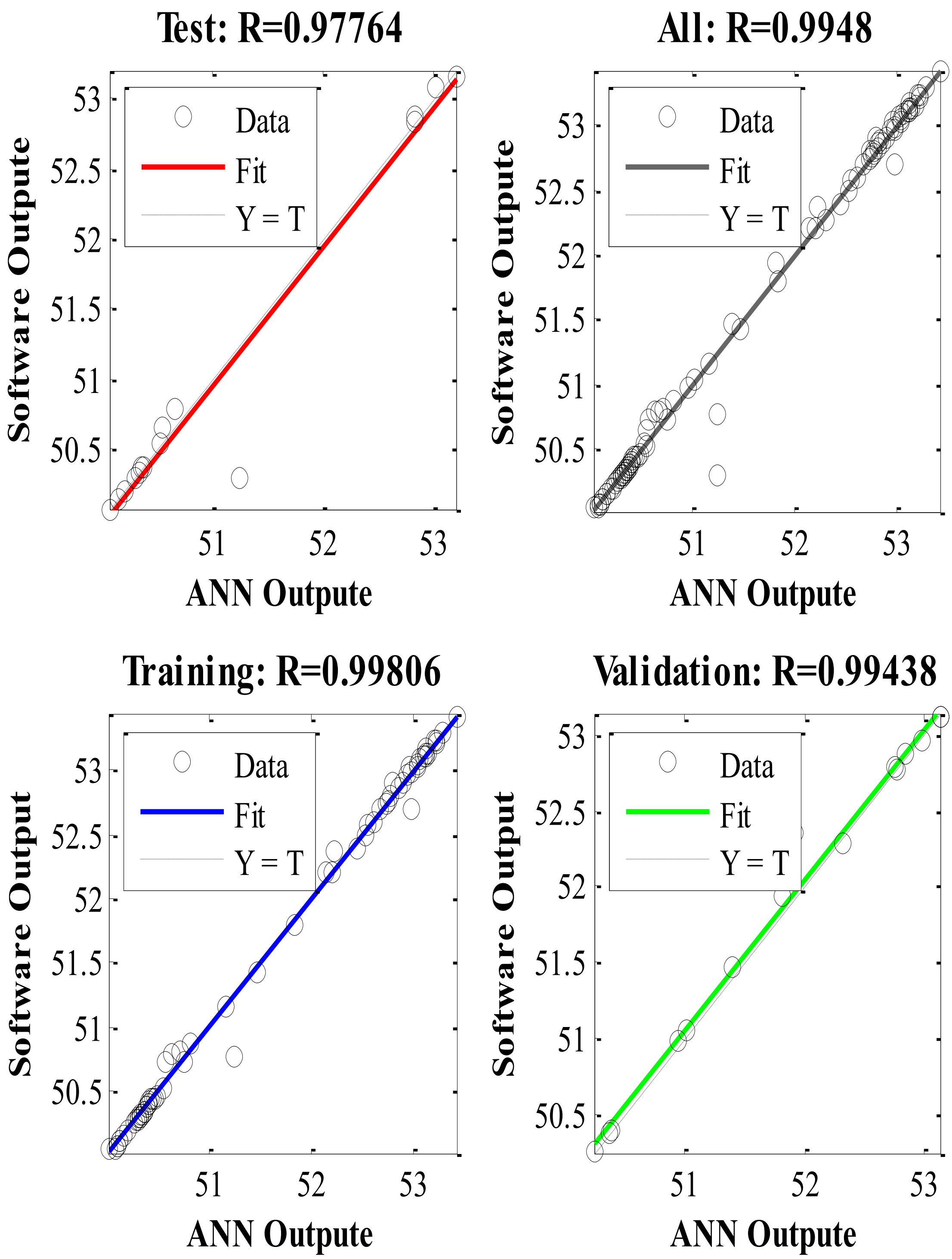

Figure 5. Linear regression for training, testing, and validation functions of the neural network utilized for predicting one-way concrete slabs' shear capacity (dimension ratio: 2)

10.57647/Jsm.2025.1704.17

It can be observed that that the neural network accurately predicted the shear capacity of concrete slabs (one-way slabs with dimension ratios of 2, 2.22, 2.5, 2.85, and 3.33). Thus, a relation was presented for predicting one-way slabs' shear capacity subjected to concentrated loading using the neural network-predicted numerical values.

4.4. ANN-based relation

Five one-way slabs with dimension ratios of 2, 2.22, 2.5, 2.85, and 3.33 were selected to present a relation for predicting one-way slabs' shear capacity subjected to concentrated loading. This range (2-3.3) was selected for the one-way slabs, because they exhibited unacceptable performance for <2 dimension ratios. Moreover, for slabs with >3.33 dimension ratios, the slab deflection exceeded the permissible value.

Hence, the upper bound was assumed to be 3.33 for the dimension ratios of the slabs.

The numerical values for slab shear capacity for different positions for applying the concentrated load on the Cartesian plane were analyzed using non-linear regression. Notably, herein, the length of the slab Ly, magnitude of the concentrated load, and mechanical properties of materials were assumed to be constant. In the curves, the horizontal axis represents the position of concentrated load applied along the slab Ly, while the vertical axis represents the numerical value of concrete shear capacity.

Besides, α denotes x (the longitudinal position of the applied concentrated load) to 1L (the slab Ly).

4.4.1. *One-way slabs with dimension ratio: 2*

Figure 6 shows the relation defined for predicting one-way slabs' shear capacity (dimension ratio: 2).

Here, the length of Ly and Lx was assumed to be 10 and 5 m, respectively.

R2 was calculated to be 0.8798 for one-way slabs (dimension ratio: 2), which shows good accuracy.

Thus, the presented relation for predicting their shear capacity can be expressed in terms of α as Eq. (3).

Remember that α represents the position of concentrated load applied along the Ly of one-way slabs.

$$V_c = -87.4\alpha^4 + 170\alpha^3 - 90.907\alpha^2 + 7.7593\alpha + 52.992 \quad (3)$$

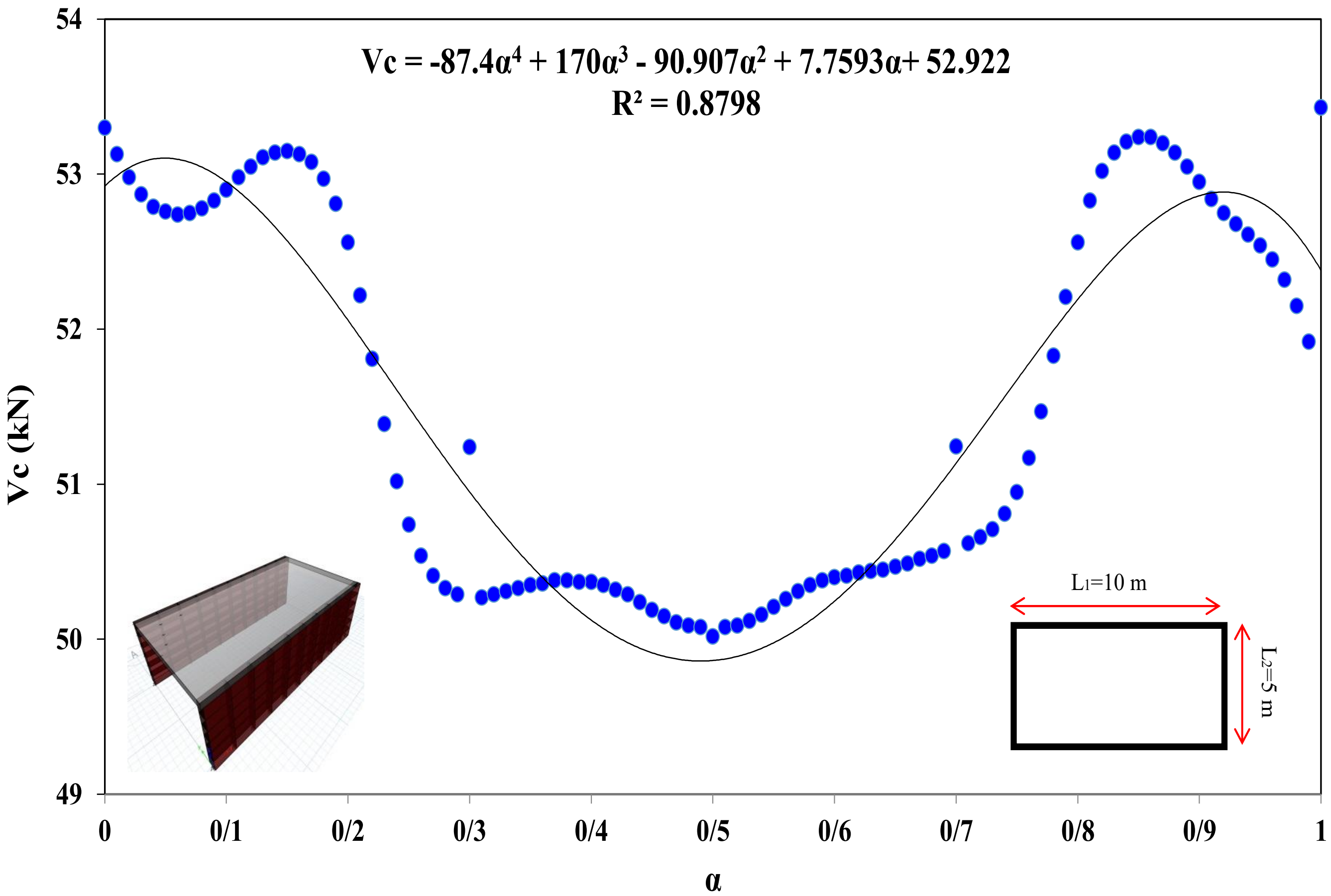

Figure 6. Relation for predicting one-way concrete slabs' shear capacity (dimension ratio: 2)

10.57647/Jsm.2025.1704.17

4.4.2. *One-way slabs with dimension ratio: 2.22*

Figure 7 shows the relation defined for predicting the one-way slabs' shear capacity (dimension ratio: 2.22). Here, the length of Ly and Lx was assumed to be 10 and 4.5 m, respectively. R2 was calculated to be 0.8798 for one-way slabs (dimension ratio: 2.22), indicating a good fit of the presented equation on points defined on the Cartesian plane. Therefore, the relation presented for predicting their shear capacity can be expressed in terms of α as Eq. (4).

$$V_c = -31.049\alpha^4 + 66.452\alpha^3 - 30.116\alpha^2 \\ -4.3675\alpha + 46.83 \tag{4}$$

4.4.3. *One-way slabs with dimension ratio: 2.5*

Figure 8 shows the formula defined for predicting one-way slabs' shear capacity (dimension ratio: 2.5). Here, the length of Ly and Lx was assumed to be 10 and 4 m, respectively.

R2 was calculated to be 0.9409 for one-way slabs (dimension ratio: 2.5), indicating a suitable fit of the presented equation on the points defined on the Cartesian plane.

Thus, the presented relation for predicting their shear capacity can be expressed in terms of α as Eq. (5).

$$V_c = -60.169\alpha^4 + 109.53\alpha^3 \\ -40.515\alpha^2 + 8.9262\alpha + 43.736 \tag{5}$$

4.4.4. *One-way slabs with dimension ratio: 2.85*

Figure 9 shows the relation defined for predicting one-way slabs' shear capacity (dimension ratio: 2.85). Here, the length of Ly and Lx was assumed to be 10 and 3.5 m, respectively. R2 was calculated to be 0.8453 for one-way slabs (dimension ratio: 2.85), indicating a good fit of the presented equation on the points defined on the Cartesian plane.

Thus, the relation presented for predicting their shear capacity can be expressed in terms of α as Eq. (6).

$$V_c = 62.889\alpha^4 - 120.14\alpha^3 + 92.086\alpha^2 \\ -34.993\alpha + 40.846 \tag{6}$$

4.4.5. *One-way slabs with dimension ratio: 3.33*

Figure 10 shows the relation defined for predicting one-way slabs' shear capacity (dimension ratio: 3.33). Here, the length of Ly and Lx was assumed to be 10 and 3 m, respectively. R2 was calculated to be 0.8723 for one-way slabs (dimension ratio: 3.33), which shows a good fit of the presented equation on the points defined on the Cartesian plane. Thus, the relation presented for predicting their shear capacity can be expressed in terms of α as Eq. (7). Remember that α represents the position of concentrated load along the Ly of one-way slabs.

$$V_c = 15.768\alpha^4 - 24.883\alpha^3 + 27.121\alpha^2 \\ -16.617\alpha + 52.791 \tag{7}$$

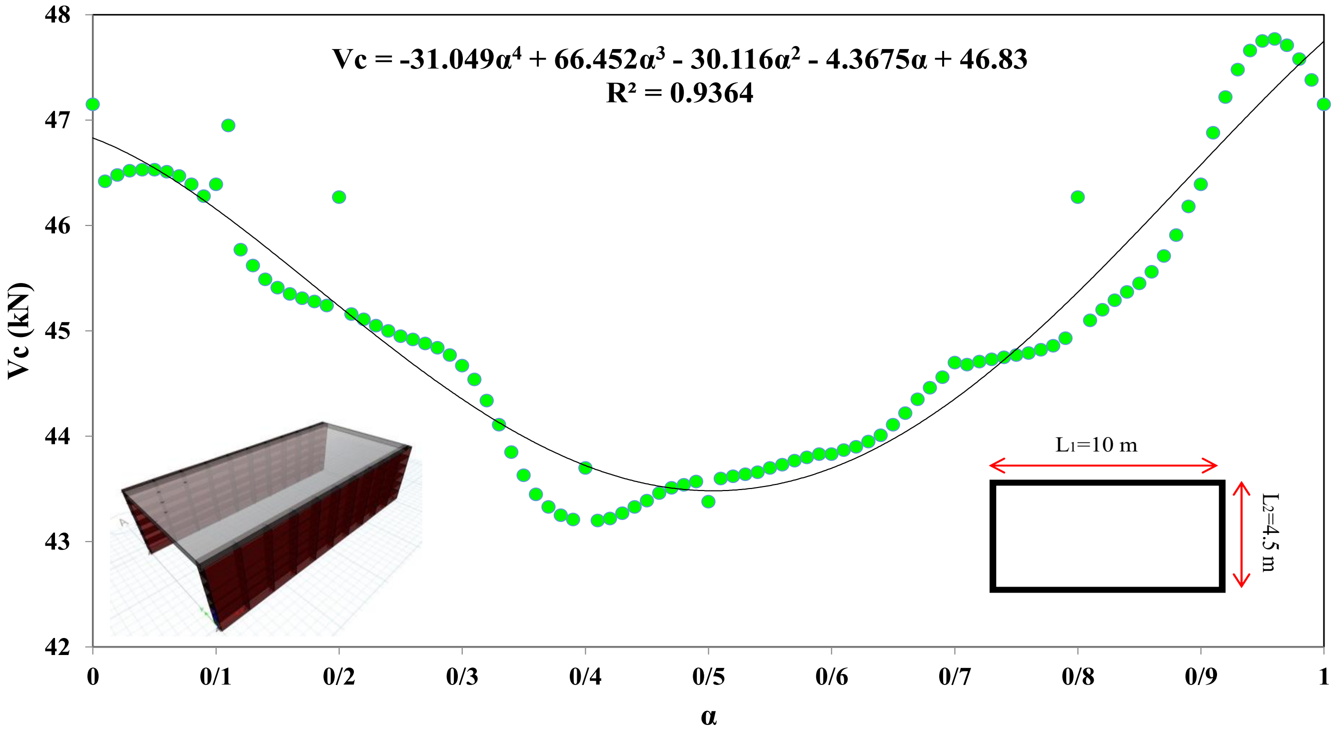

Figure 7. Relation for predicting one-way concrete slabs' shear capacity (dimension ratio: 2.22)

10.57647/Jsm.2025.1704.17

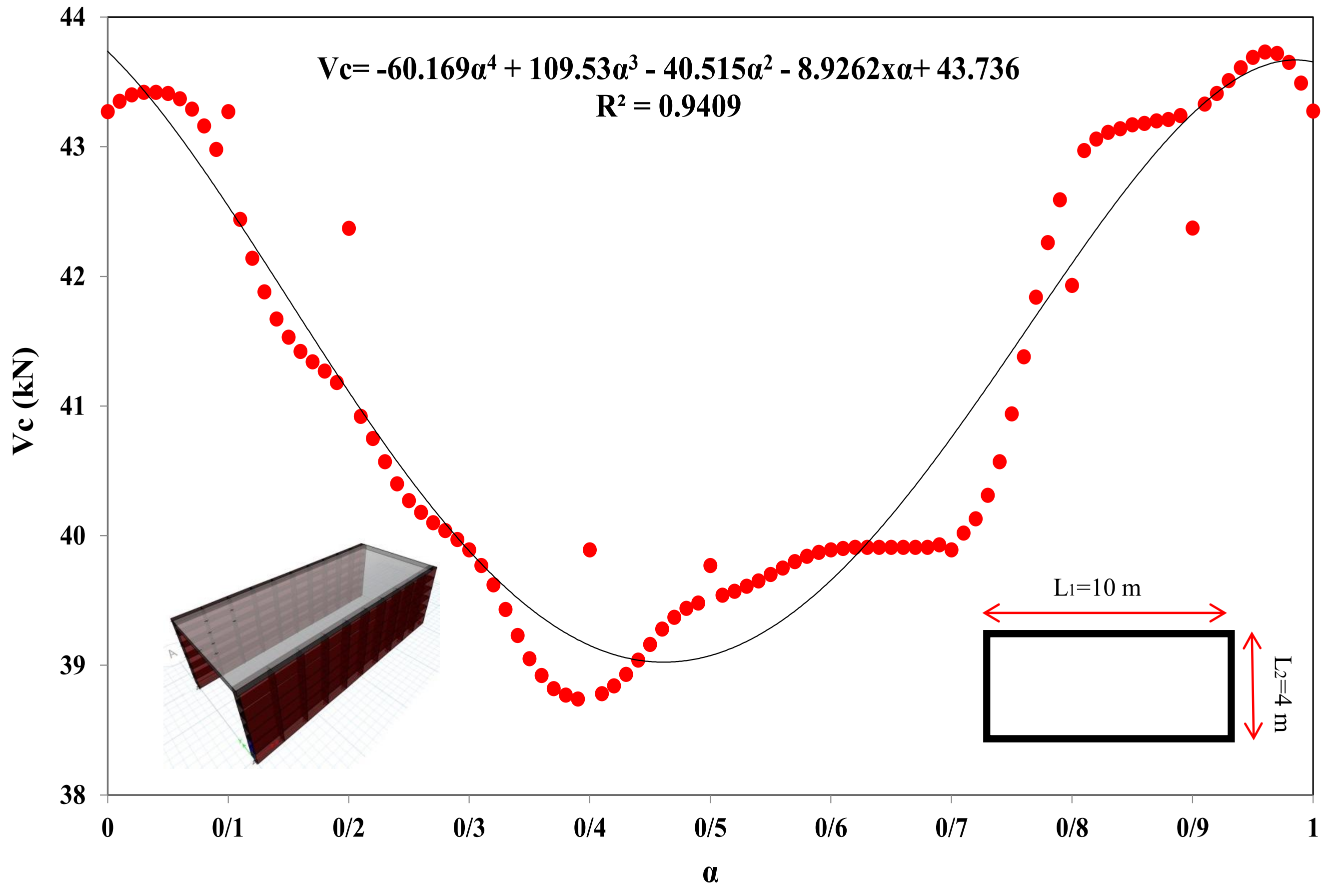

Figure 8. Relation for predicting one-way concrete slabs' shear capacity (dimension ratio: 2.5)

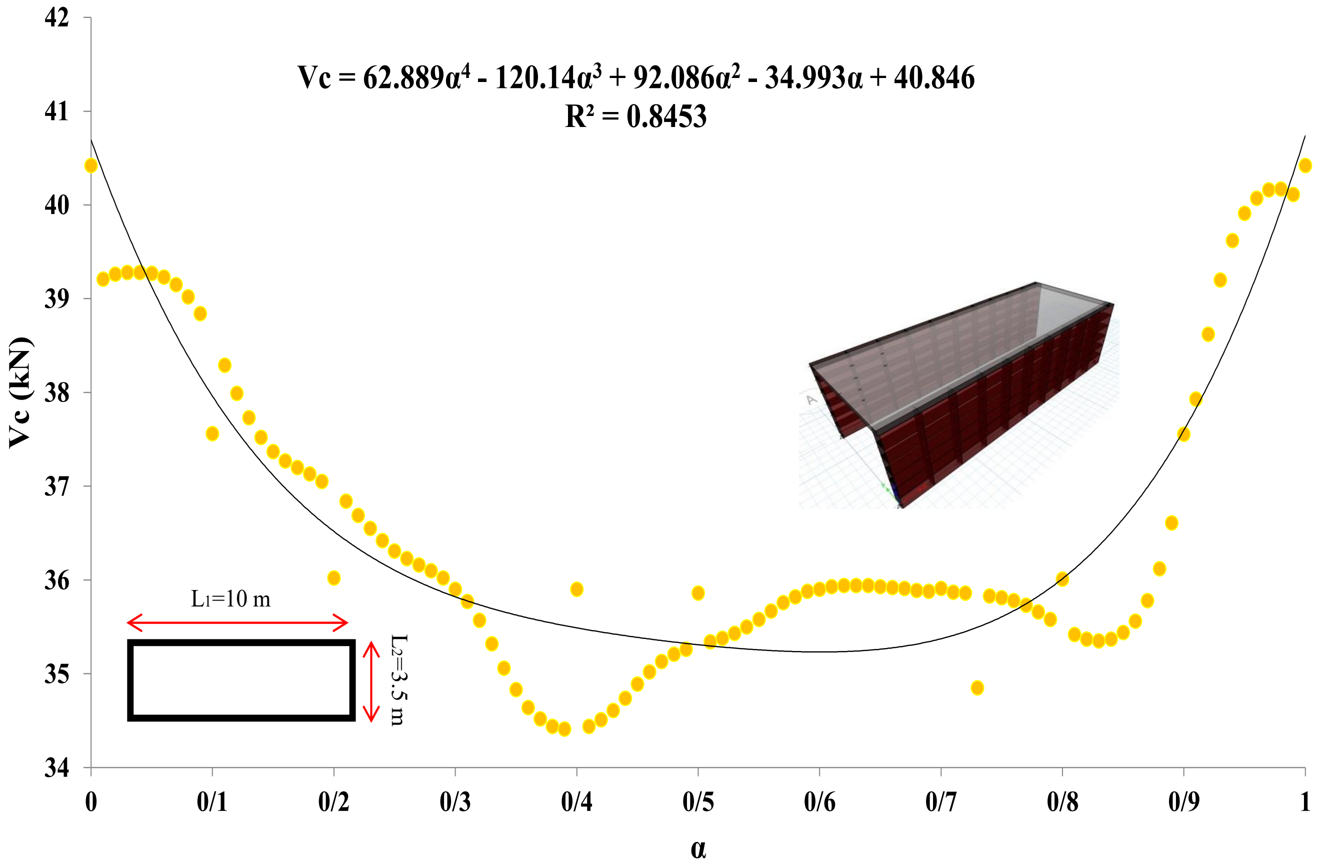

Figure 9. Relation for predicting one-way concrete slabs' shear capacity (dimension ratio: 2.85)

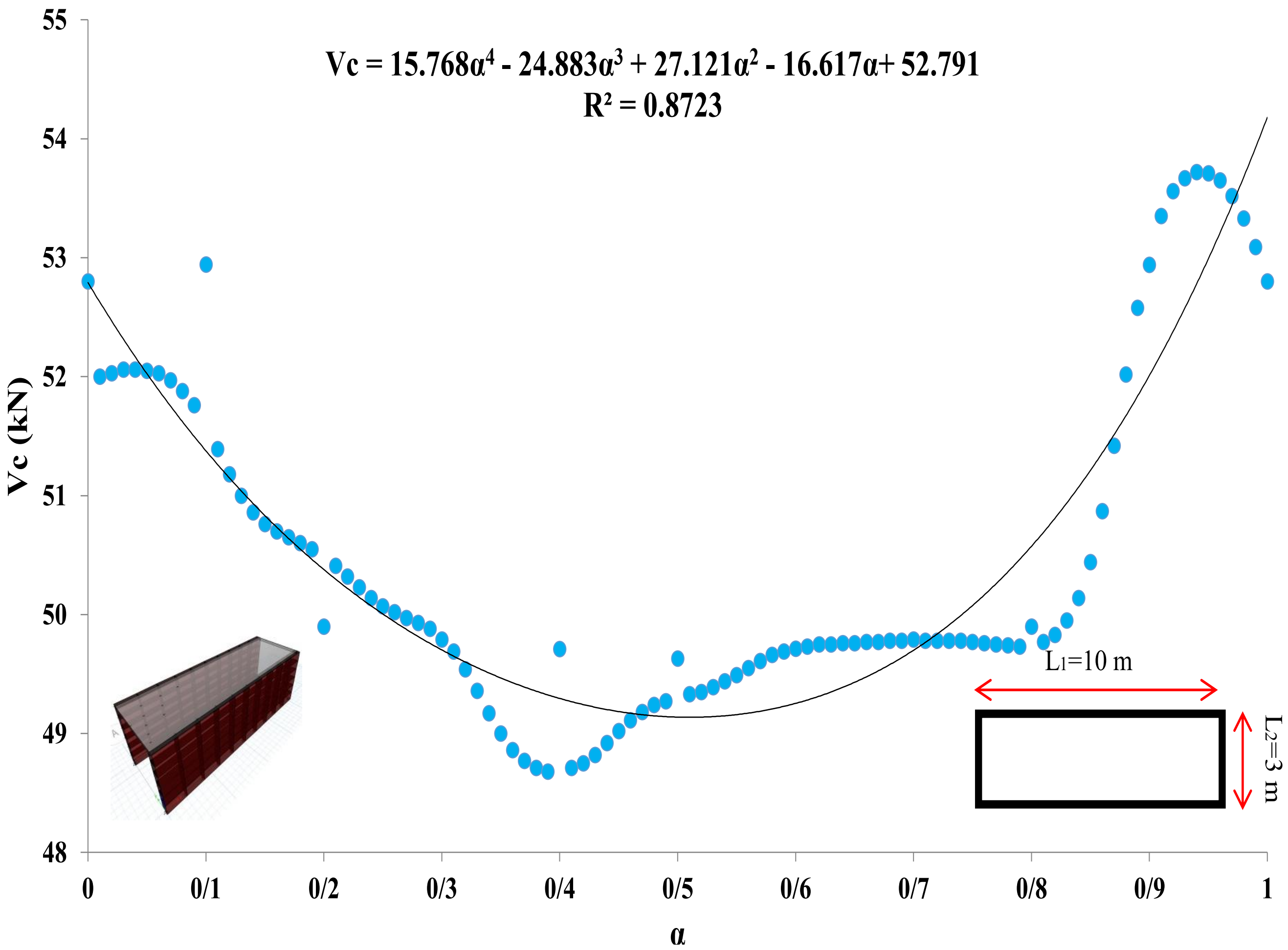

Figure 10. Relation for predicting one-way concrete slabs' shear capacity (dimension ratio: 3.33)

It should be noted that Eqs. 3 to 7 present the shear capacity of a one-way slab with different dimension ratios in terms of α with high accuracy, so that these relations greatly facilitate the modeling process of one-way slabs within the specified range and have the ability to be generalized to more diverse configurations (within the range of dimension ratios of 2 to 3.33). In other words, by substituting the numerical value of the dimension ratio of the one-way slab in these relations, the shear capacity of the slab can be achieved with high accuracy, which in practice increases the speed of calculations and prevents wasting time on difficult modeling. According to the results regarding the formula presented for predicting one-way slabs' shear capacity for different dimension ratios, the relation for predicting one-way slabs' shear capacity subjected to concentrated loading can be expressed as Eq. (8). Table 5 lists the coefficients A, B, C, D, and E with different numerical values for different dimension ratios.

$$V_c = A\alpha^4 - B\alpha^3 + C\alpha^2 - D\alpha + E \tag{8}$$

Figure 11 shows the fitting and linear regression of A, B, C, D, and E for α so as to provide a general relation for predicting one-way slabs' shear capacity. As per the coefficients listed in Table 6, the general relation for predicting one-way slabs' shear capacity subjected to concentrated loading can be expressed as Eq. (9).

$$V_c = 86.197\alpha^4 - 164.64\alpha^3 + 101.11\alpha^2 - 21.777\alpha + 38.89 \tag{9}$$

5. Verification of the relation

This section verifies the relation presented for predicting one-way slabs' shear capacity to ensure its accuracy. For this purpose, a one-way concrete slab [dimension ratio: 2.1] (length of Ly: 10.5 m; length of Lx: 5 m; thickness: 25 cm) under a single load of 15 kN at a distance of 3.675 m from the corner of the slab (α=0.35). According to the ETABS results (Figure 12), while one-way concrete slab's shear capacity was found to be 39.3 kN, it was calculated to be 37.88 kN by Eq. (9).
Therefore, it can be seen a difference of 3.61%, That is to say, the proposed relation shows an accuracy of 96.39% (Table 7).

10.57647/Jsm.2025.1704.17

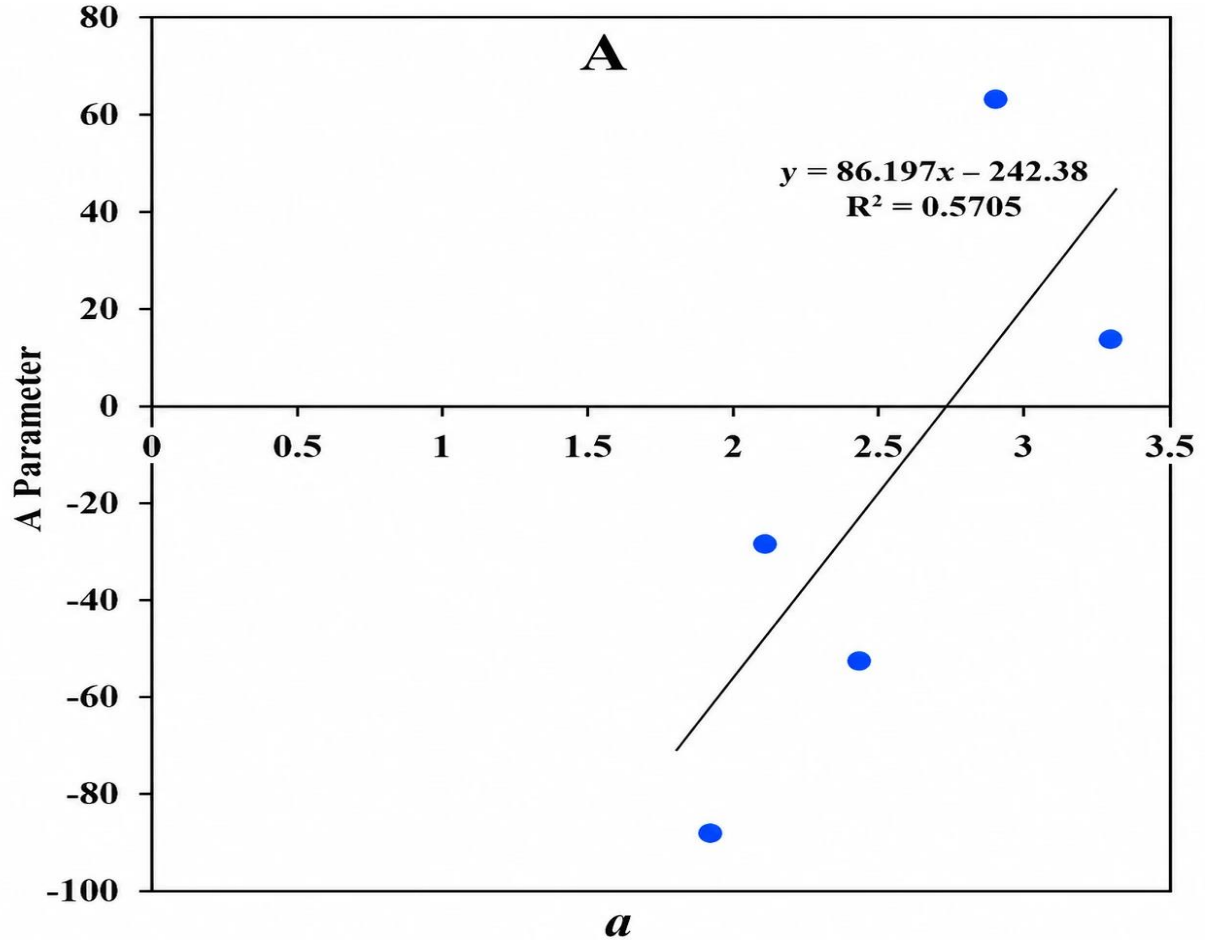
A
y = 86.197x – 242.38
R² = 0.5705
A Parameter
80
60
40
20
0
-20
-40
-60
-80
-100
0
0.5
1
1.5
2
2.5
3
3.5
a

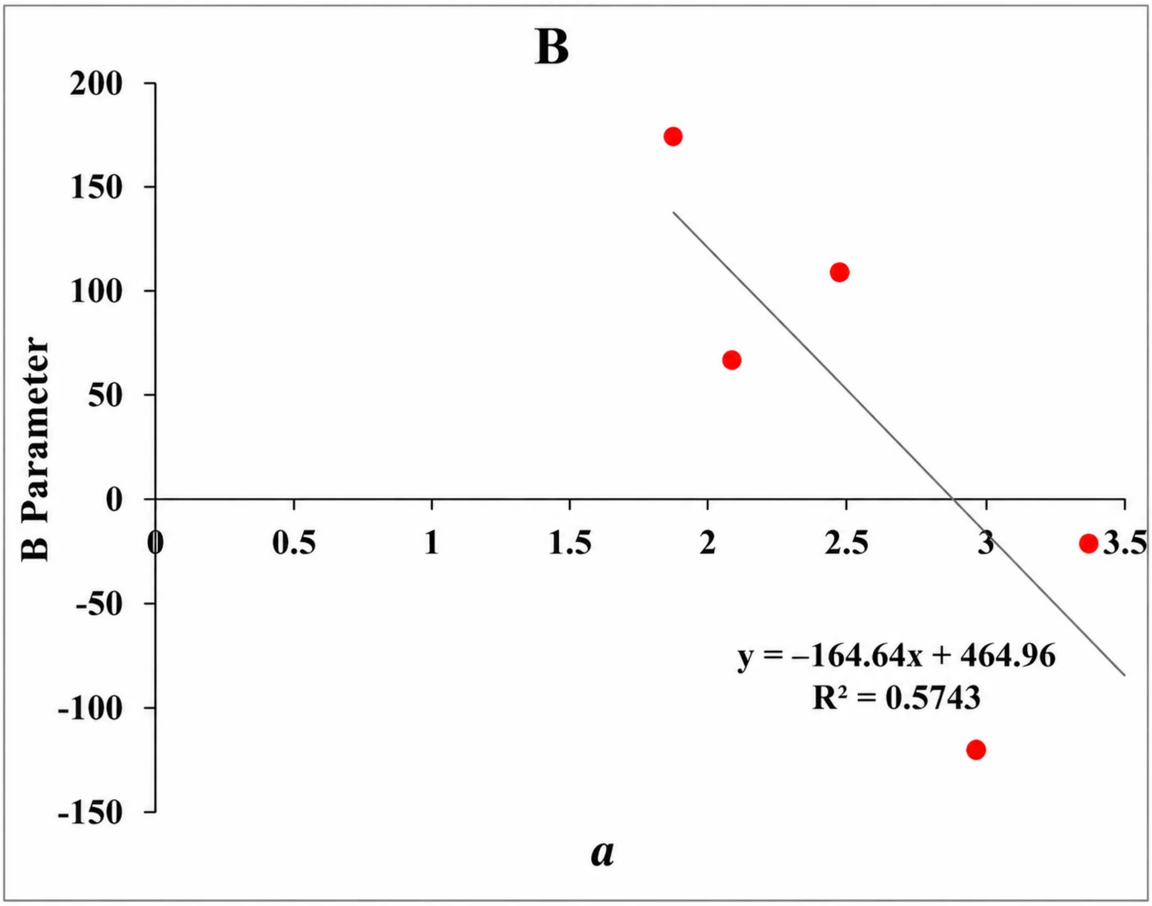
B
y = –164.64x + 464.96
R² = 0.5743
B Parameter
200
150
100
50
0
-50
-100
-150
0
0.5
1
1.5
2
2.5
3
3.5
a

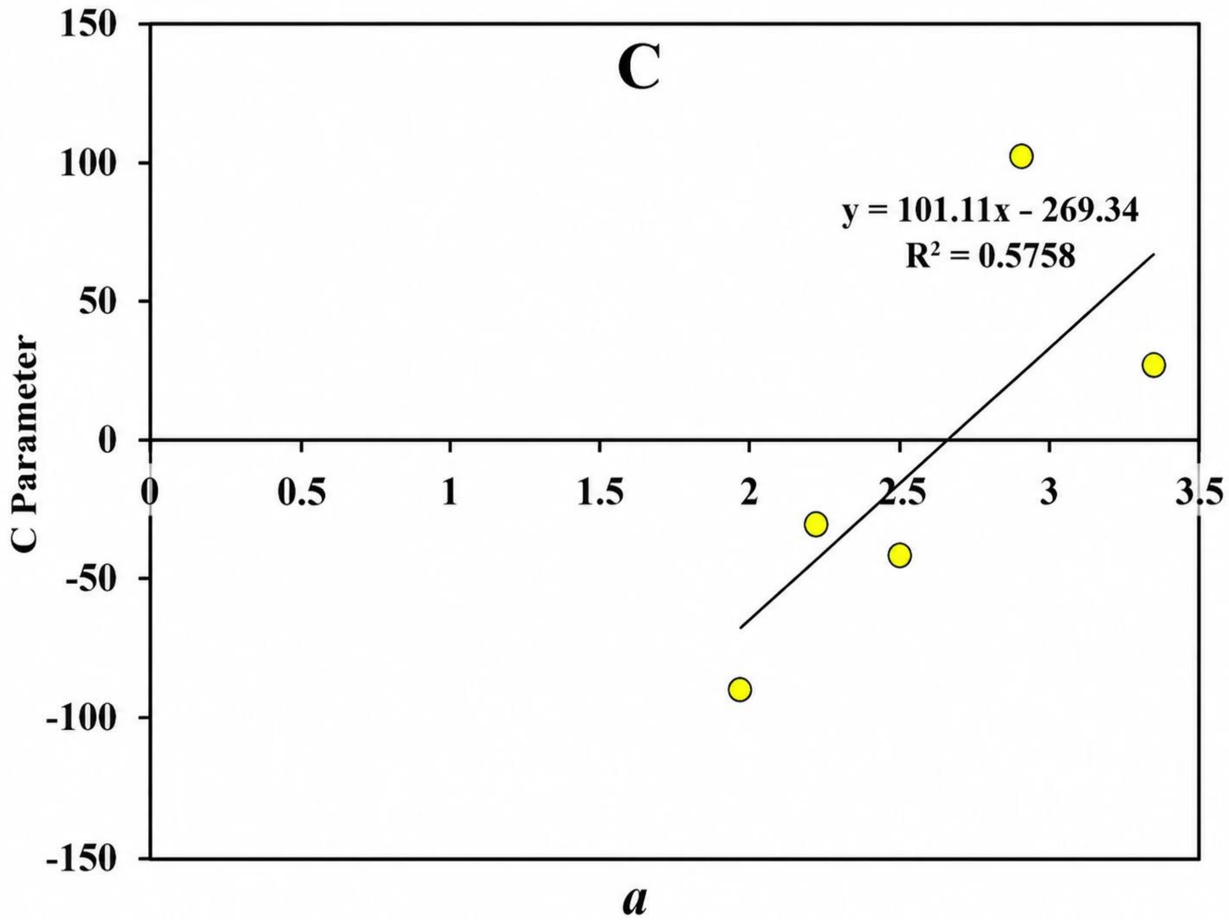

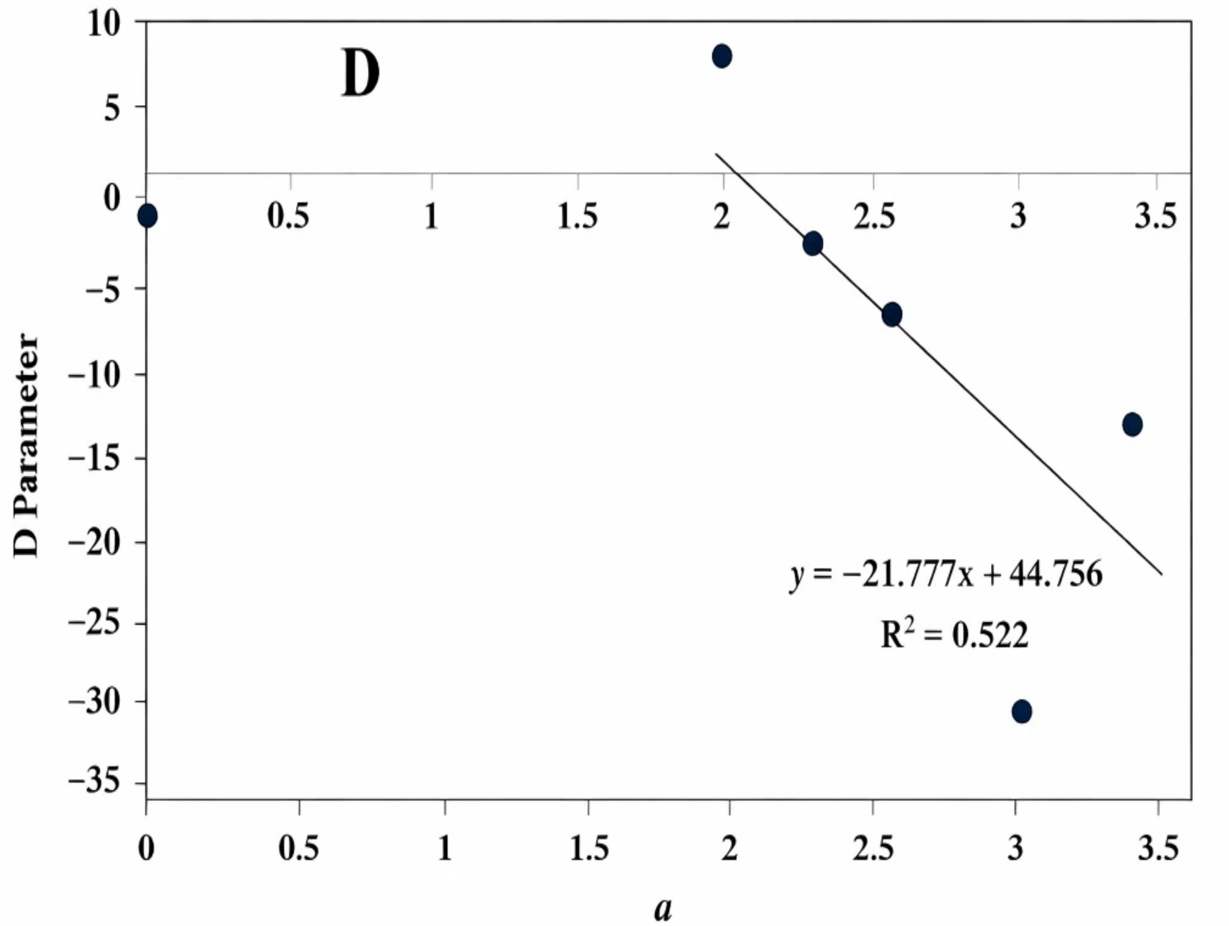

10.57647/Jsm.2025.1704.17

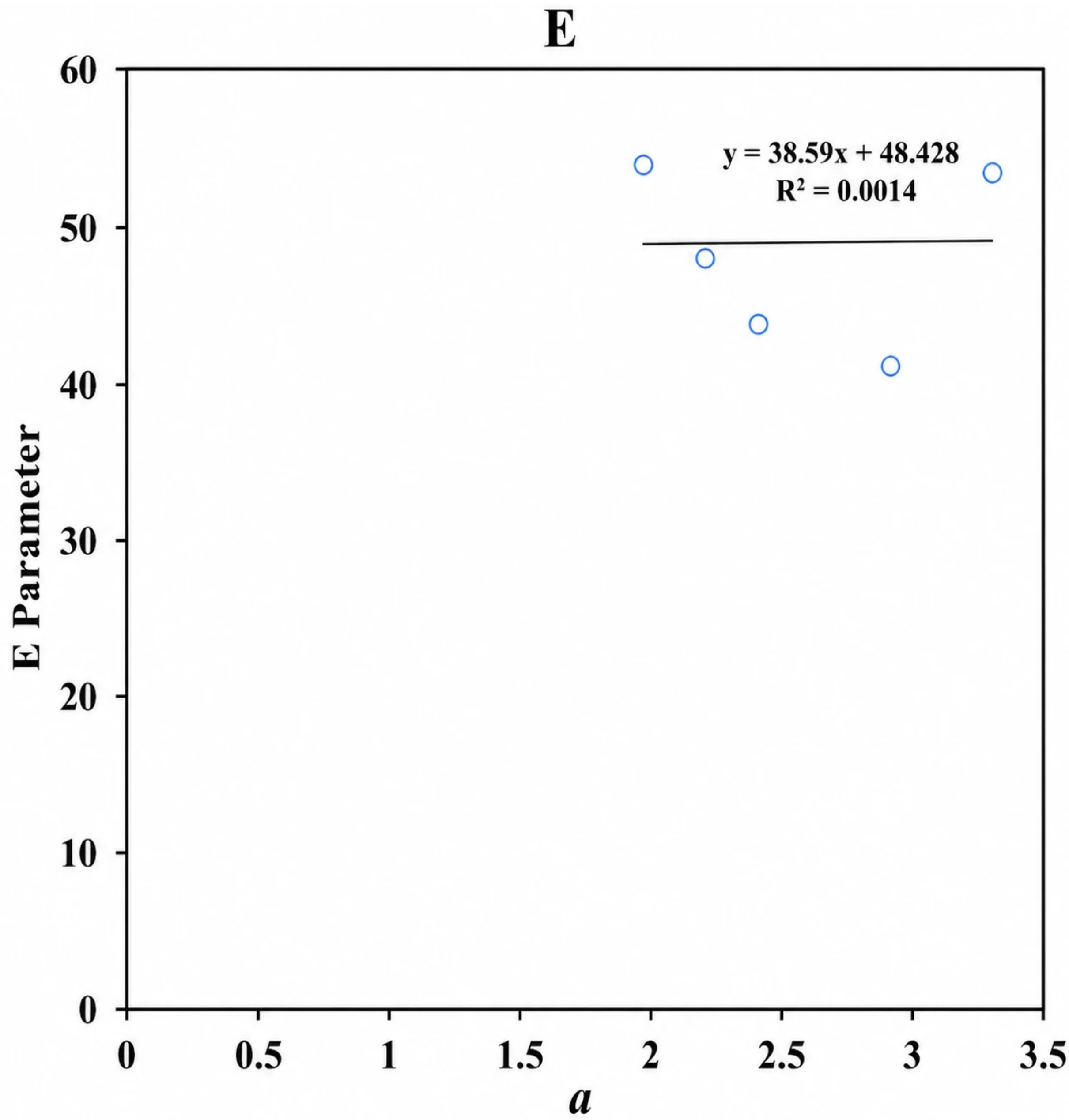

Figure 11. General relation for predicting one-way slabs' shear capacity

Table 5. Resulted coefficients to determine the equation for predicting the one-way slab's the shear capacity for different dimension ratios

L_1/L_2	A	B	C	D	E
2	-87.4	170	-90.907	7.7593	52.922
2.22	-31.049	66.452	-30.116	-4.3675	46.83
2.5	-60.169	109.53	-40.515	-8.9262	43.736
2.85	62.889	-120.14	92.086	-34.993	40.846
3.33	15.768	-24.883	27.121	-16.617	52.791

Table 6. Resulted coefficients to determine the equation for predicting one-way slabs' shear capacity

	A'	B'	C'	D'	E'
Numerical value	86.197	-164.64	101.11	21.777	38.89

10.57647/Jsm.2025.1704.17

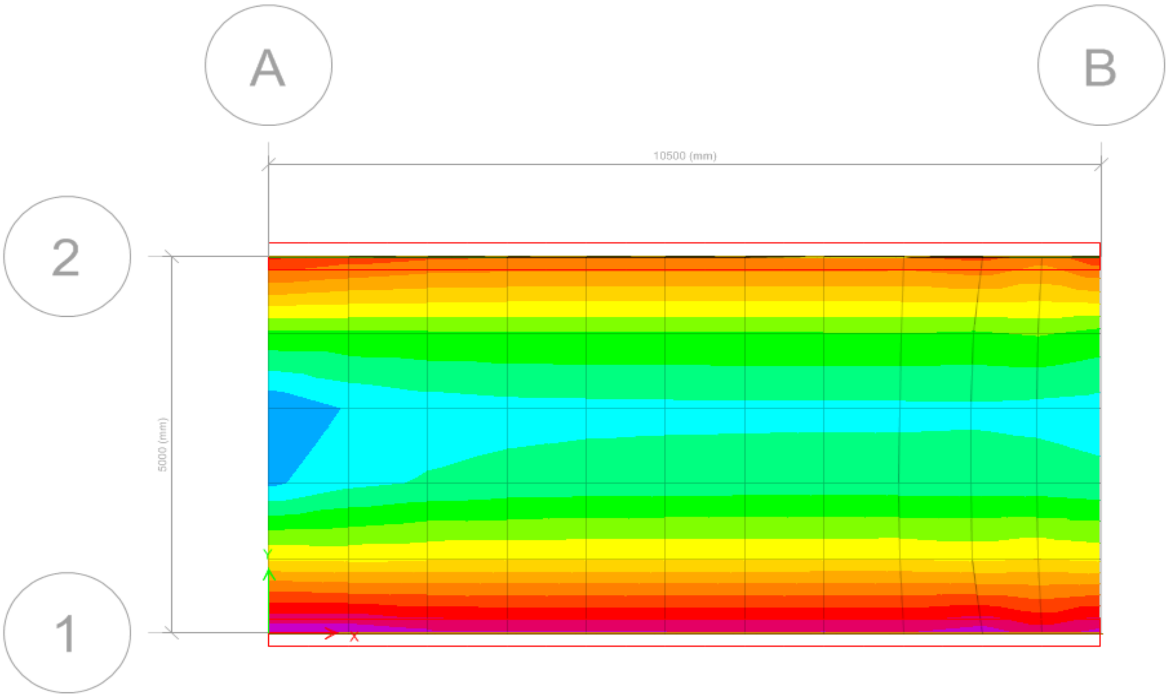

Figure 12. one-way slab shear capacity (dimension ratio: 2.1)

Table 7. Verification of Eq. (9) for predicting one-way slabs' shear capacity

Sample	Shear capacity by ETABS (kN)	Shear capacity by Eq. (9)	Difference in results (%)
One-way slab (aspect ratio: 2.1)	39.3	37.88	3.61

6.Conclusions

This research mainly aimed to present an ANN-based relation for predicting one-way slabs' shear capacity subjected to concentrated loads. To this aim, five one-way slabs with different dimension ratios (ranging from 2 to 3.3) were modelled by ETABS, and their shear capacity was calculated following the application of concentrated load along the Ly (for 11 different positions). To control the deflection in the modelled slabs, the maximum [allowable] slab deflection was compared with the permissible value determined in the ACI Code. A neural network was then employed for predicting concrete slabs' shear capacity, which was then trained by data derived from ETABS.

Afterward, shear capacity was predicted for all five slabs using the neural network method in MATLAB. The predicted accuracy was evaluated based on the regression coefficient. In the next step, an equation was defined for each studied slab to calculate concrete slabs' load-bearing capacity based on the positions of applying the concentrated load.

A general relation was then presented by data fitting and linear regression to determine concrete slabs' load-bearing capacity for α (the concentrated load application position). To evaluate the accuracy of the presented general relation, shear capacity was calculated by ETABS for a one-way slab and compared with the numerical value obtained from the proposed relation.

For future research, it is recommended to use nonlinear finite element modeling and experimental data. It is also recommended to use larger datasets (experimental or numerical) to generalize the results and make more accurate comparisons.

The most important conclusions drawn from this study include:

- ✓ Concentrated loads were assumed to be constant. One-way slabs (dimension ratio >3.33) were excluded from the list of modelled slabs due to the deflection exceeding the allowable limit specified in the ACI Code.
  For this purpose, in Table (2), the largest slab aspect ratio is considered to be 3.33 and larger ratios are not considered.
- ✓ The most optimum neural network topology for predicting one-way slabs' shear capacity was to use two hidden intermediate layers and 10 neurons per layer.
- ✓ In general, a fourth-order nonlinear equation was proposed for predicting one-way slabs' shear capacity subjected to concentrated loading:

$$V_c = A\alpha^4 - B\alpha^3 + C\alpha^2 - D\alpha + E$$

10.57647/Jsm.2025.1704.17

✓ Shear capacity can be determined for concrete one-way slabs (dimension ratio: 2-3.3) under constant concentrated loads by the following equation:

$$V_c = 86.197\alpha^4 - 164.64\alpha^3 + 101.11\alpha^2$$
$$-21.777\alpha + 38.89$$

✓ The general relation presented for a concrete slab (dimension ratio: 2.1) under a 15kN concentrated load at a relative distance of 0.35 from the corner of the slab Ly obtained an accuracy of 96.39%.

Authors Contribution

The simulations and paper draft writing are performed by Ali Akbari. The paper is completed by Dr. Ashkan Khodabandehlou and results are discussed with Dr. Fedra Ashrafzadeh and Dr. Peyman Hamidi.

Availability of data and materials

All data generated or analysed during this study are included in this published article.

Conflict of interests

The authors state that they have not any conflict of interest.

References

[1] Shen, Y., Sun, J., and Liang, S (2022). Interpretable Machine Learning Models for Punching Shear Strength Estimation of FRP Reinforced Concrete Slabs, Crystals, vol. 12, no.2.

[2] Lantsoght, E. O. L., Van Der Veen, C., and De Boer, A (2017). Extended Strip Model for slabs subjected to load combinations, Eng. Struct., vol. 145, pp. 60–69.

[3] Lantsoght, E. O. L., Van Der Veen, C., De Boer, A., and Walraven, J. C (2015). One-way slabs subjected to combination of loads failing in shear, ACI Struct. J., vol. 112, no. 4, pp. 419–428.

[4] Lantsoght, E. O. L., Van Der Veen, C., De Boer, A,, and Walraven, J. C (2014). Influence of width on shear capacity of reinforced concrete members, ACI Struct. J., vol. 111, no. 6, pp. 1441–1449.

[5] Hoang, N. D (2019). Estimating punching shear capacity of steel fibre reinforced concrete slabs using sequential piecewise multiple linear regression and artificial neural network. Meas. J. Int. Meas. Confed., vol. 137, pp. 58–70.

[6] Alkroosh, I., and Ammash, H (2015). Soft computing for modeling punching shear of reinforced concrete flat slabs, Ain Shams Eng. J., vol. 6, no. 2, pp. 439–448.

[7] American Concrete Institute. ACI 440.2R-08, Building code requirements for structural concrete and commentary. 2011.

[8] BSI (British Standards Institution), Structural use of concrete, 2005.

[9] Thomas Telford Ltd. London, CEP-FIP Model Code, 1993.

[10] Aggarwal, Y., Aggarwal, P., Sihag, P., Pal, M., and Kumar, A (2019). Estimation of punching shear capacity of concrete slabs using data mining techniques, Int. J. Eng. Trans. A Basics, vol. 32, no. 7, pp. 908–914.

[11] Elshafey, A.A., Rizk, E., Marzouk, H., and Haddara, M.R(2011). Prediction of punching shear strength of two-way slabs, Eng. Struct., vol. 33, no. 5, pp. 1742–1753, 2011.

[12] Elshafey, A.A., Haddara, M.R., and Marzouk, H (2010). Damage detection in offshore structures using neural networks, Mar. Struct., vol. 23, no. 1, pp. 131–145.

[13] Shu, J.P., Bagge, N., Plos,M., Johansson, M, Yang,Y., and Zandi, K (2018). Shear Capacity of a RC Bridge Deck Slab: Comparison between Multilevel Assessment and Field Test, Journal of structural enginnering vol. 144, no. 7, pp. 1–16.

[14] Belletti, B., Damoni, C., Hendriks, M., and Uijl, J (2020). Nonlinear finite element analyses of reinforced concrete slabs: comparison of safety formats 1 introduction.

[15] Lantsoght, E. O. L., Van Der Veen, C., and Walraven, J.C (2014). Shear in One-Way Slabs under Concentrated Load Close to Support, no. 110, pp. 275–284.

[16] Liu, Ch., Guo, S. (2024). Vertical shear capacity of steel-normal concrete-UHPC composite slabs with steel ribs in the cantilever, Structures 64.

[17] Truong, D.N., To,V., Truong,G., Seung Jang,H. (2024). Engineering punching shear strength of flat slabs predicted by nature-inspired metaheuristic optimized regression system, Frontiers of Structural and Civil Engineering 18, pp551-567.

[18] Cao,Ch., Hu,Zh.,Chai,Y., Li,Q., Li,W, Pan,H and Li,Y (2024). Investigations on interface shear-stress transfer behavior of concrete composite slabs with lattice girders, KSCE Journal of Civil Engineering 28(10), pp

4457-4472.

[19] Shirkhani, A., Davarnia, D., Azar, B. F. (2019). Prediction of bond strength between concrete and rebar under corrosion using ANN. Computers and Concrete, An International Journal, 23(4), 273-279.

[20] Nouri, Y., Ghanizadeh, A. R., Jahanshahi, F. S., Fakharian, P. (2025). Data-driven prediction of axial compression capacity of GFRP-reinforced concrete column using soft computing methods   Journal of Building Engineering , 101, 111831.

[21] Chen, L., Fakharian, P., Eidgahee, D. R., Haji, M., Arab, A. M. A., Nouri, Y. (2023). Axial compressive strength predictive models for recycled aggregate concrete filled circular steel tube columns using ANN, GEP, and MLR. Journal of Building Engineering, 77, 107439.

[22] Fakharian, P., Nouri, Y., Ghanizadeh, A. R., Jahanshahi, F. S., Naderpour, H., Kheyroddin, A. (2024). Bond strength prediction of externally bonded reinforcement on groove method (EBROG) using MARS-POA. Composite Structures, 349, 118532.

[23] Ammari, A. S., Nouri, Y., Jouneghani, H. G., Hosseini, S. A., Rayegani, A., Ebrahimi, M., Heydari, P. (2025). Flexural strengthening of corroded steel beamswith CFRP by using the end anchorage: Experimental, numerical, and machine learning methods. Case Studies in Construction Materials, e04966.

[24] Chen, L., Nouri, Y., Allahyarsharahi, N., Naderpour, H., Rezazadeh Eidgahee, D., Fakharian, P. (2025). Optimizing compressive strength predictionin eco-friendly recycled concrete via artificial intelligence models. Multiscale and Multidisciplinary Modeling, Experiments and Design, 8(1), 24.

[25] Nouri, Y., Ghanbari, M. A., Fakharian, P. (2024). An integrated optimization and ANOVA approach for reinforcing concrete beams with glass fiber polymer. Decision Analytics Journal, 11, 100479.